

Article

Mechanistic Thermal Modeling of Late Triassic Terrestrial Amniotes Predicts Biogeographic Distribution

Scott A. Hartman ^{1,*}, David M. Lovelace ², Benjamin J. Linzmeier ³, Paul D. Mathewson ¹
and Warren P. Porter ¹

¹ Department of Integrative Biology, University of Wisconsin-Madison, Madison, WI 53706, USA

² Geology Museum, Department of Geosciences, University of Wisconsin-Madison, Madison, WI 53706, USA

³ Department of Earth Sciences, University of South Alabama, Mobile, AL 36688, USA

* Correspondence: sahartman@wisc.edu

Abstract: The biogeography of terrestrial amniotes is controlled by historical contingency interacting with paleoclimate, morphology and physiological constraints to dispersal. Thermal tolerance is the intersection between organismal requirements and climate conditions which constrains modern organisms to specific locations and was likely a major control on ancient tetrapods. Here, we test the extent of controls exerted by thermal tolerance on the biogeography of 13 Late Triassic tetrapods using a mechanistic modeling program, Niche Mapper. This program accounts for heat and mass transfer into and out of organisms within microclimates. We model our 13 tetrapods in four different climates (cool and warm at low and high latitudes) using environmental conditions that are set using geochemical proxy-based general circulation models. Organismal conditions for the taxa are from proxy-based physiological values and phylogenetic bracketing. We find that thermal tolerances are a sufficient predictor for the latitudinal distribution of our 13 test taxa in the Late Triassic. Our modeled small mammaliamorph can persist at high latitudes with nocturnal activity and daytime burrowing but large pseudosuchians are excluded because they cannot seek nighttime shelter in burrows to retain elevated body temperatures. Our work demonstrates physiological modeling is useful for quantitative testing of the thermal exclusion hypothesis for tetrapods in deep time.

Keywords: paleoecology; Triassic; Niche Mapper; biogeography; thermal modeling



Citation: Hartman, S.A.; Lovelace, D.M.; Linzmeier, B.J.; Mathewson, P.D.; Porter, W.P. Mechanistic Thermal Modeling of Late Triassic Terrestrial Amniotes Predicts Biogeographic Distribution. *Diversity* **2022**, *14*, 973. <https://doi.org/10.3390/d14110973>

Academic Editor: Octávio Mateus

Received: 27 September 2022

Accepted: 9 November 2022

Published: 12 November 2022

Publisher's Note: MDPI stays neutral with regard to jurisdictional claims in published maps and institutional affiliations.



Copyright: © 2022 by the authors. Licensee MDPI, Basel, Switzerland. This article is an open access article distributed under the terms and conditions of the Creative Commons Attribution (CC BY) license (<https://creativecommons.org/licenses/by/4.0/>).

1. Introduction

All organisms, living or extinct, exist within the physical constraints placed on them by their environments. These constraints include material properties, gravity and more complex but equally important thermodynamic interactions. The derivation of heat and mass-balance equations from experimental data and first principles make it possible to model the thermal interactions of organisms with their environments [1–3]. In extant organisms mechanistic niche modeling successfully predicts temperature preference, habitat selection, range extension, and food requirements of animals across a wide range of size and phylogenetic diversity [2,4–7].

Anticipating future work on extinct organisms, Porter and Gates [8] explored the role of size and insulation in modulating temperature fluctuations in hypothetical tetrapods from a few grams up to 100 kg. Using a modified form of their heat-transfer equations, Spotila et al. [9] investigated the role size plays in damping the impact of external temperature change on thermoregulation in hypothetical giant ectotherms, which they extrapolated to infer that ectothermic non-avian dinosaurs could achieve functionally homeothermic core temperature as long as they lived in the warm, stable climatic regimes [10].

Dunham et al. [11] applied a more sophisticated microclimate model to the Late Cretaceous hadrosaur *Maiasaura* while investigating the role of size and life history strategy in dinosaur thermoregulation. While confirming the importance increasing mass plays

in insulating an organism from temperature change, their whole-body heat generation and counter-current heat exchange model demonstrated that average body temperatures in ~5 tonne ectotherms would have been lower than those calculated by Spotila et al. [9] and would not have produced elevated, homeothermic body temperatures.

Though the use of mechanistic modeling to investigate thermal ecology in extant ecosystems has steadily made advancements with extant taxa [4,12,13], investigations into Mesozoic faunas halted after Dunham et al. [11] until recently [14]. Recent advances in multi-proxy reconstruction of local paleoclimates and improved global climate modeling (GCMs) provide a robust basis to utilize mechanistic modeling to investigate thermal ecology in Mesozoic ecosystems [14–16], while continued refinement of thermal modeling may conversely allow fossil vertebrates to one day serve as viable constraints on climate modeling [17–19].

Here, we utilized a series of microclimate models to investigate the thermal ecology of thirteen representative terrestrial Late Triassic amniotes at high and low latitudes in both seasonally wet (monsoonal) and arid climates. Our modeled results demonstrate the presence or absence of thermal stress are consistent with the actual paleobiogeographic distributions of major terrestrial amniote clades in the Late Triassic. Given the importance of this interval of time to the rise of the modern fauna—which includes turtles, mammals, crocodiles, and birds—it is critical to understand the role thermoregulation played during the evolution of these disparate clades across variable physiological regimes, paleogeography, and life histories.

2. Materials and Methods

We employed the mechanistic thermal modeling program Niche Mapper™ [20]. Niche Mapper combines user inputted microclimate models with biophysical organismal models to calculate heat and mass balance solutions for an organism within its environment hourly, for multiple years [18]. The core of Niche Mapper is a Fortran program compiled into an executable with up to five input files and three output files. To increase the efficiency of modeling dozens of species in multiple environments, we wrote an R script that populates the input text files, initiates Niche Mapper, and compiles the results into a single data frame for analysis [14,21].

Plotting of compiled results utilized the R packages PNG [22]; gplots [23]; ggplot2 [24]; RColorBrewer [25]; and Plotrix [26]. Paleobiogeographic ranges were evaluated using the Paleobiology Database (paleobiodb.org). Outcrop data was obtained from the Macrostratigraphy Database (macrostrat.org). Paleogeographic reconstruction and rotation of fossil occurrences and outcrop area utilized Gplates (gplates.org), and maps were plotted using QGIS [27].

2.1. Microclimate Models

Niche Mapper's microclimate model uses 49 user-inputted fields to define maximum and minimum wind speed, air temperature, humidity, cloud cover, shade, and soil properties, and seasonal variations thereof (Figure 1; See Appendix S1 of Lovelace et al., 2020 for the complete list). Insolation is independently calculated based on latitude, longitude, elevation, and time of year [28]) in the palinsol R package [29]. For a given model day, Niche Mapper fits a sinusoidal curve to inputted minimum and maximum macroclimate values of air temperature, relative humidity, wind speeds, and cloud cover to provide hourly profiles. These data are also used to compute vertical profiles from ground level to 2 m height of air temperature, relative humidity and wind speed to provide microclimate conditions at the height of the model animal. We set maximum air temperature and wind speed, and minimum relative humidity and cloud cover to occur one hour after solar noon [30]. Computed solar radiation reaching the ground varies according to time of year, hour of day, latitude, elevation, cloud cover and the potential to seek shade and/or burrows [31–33].

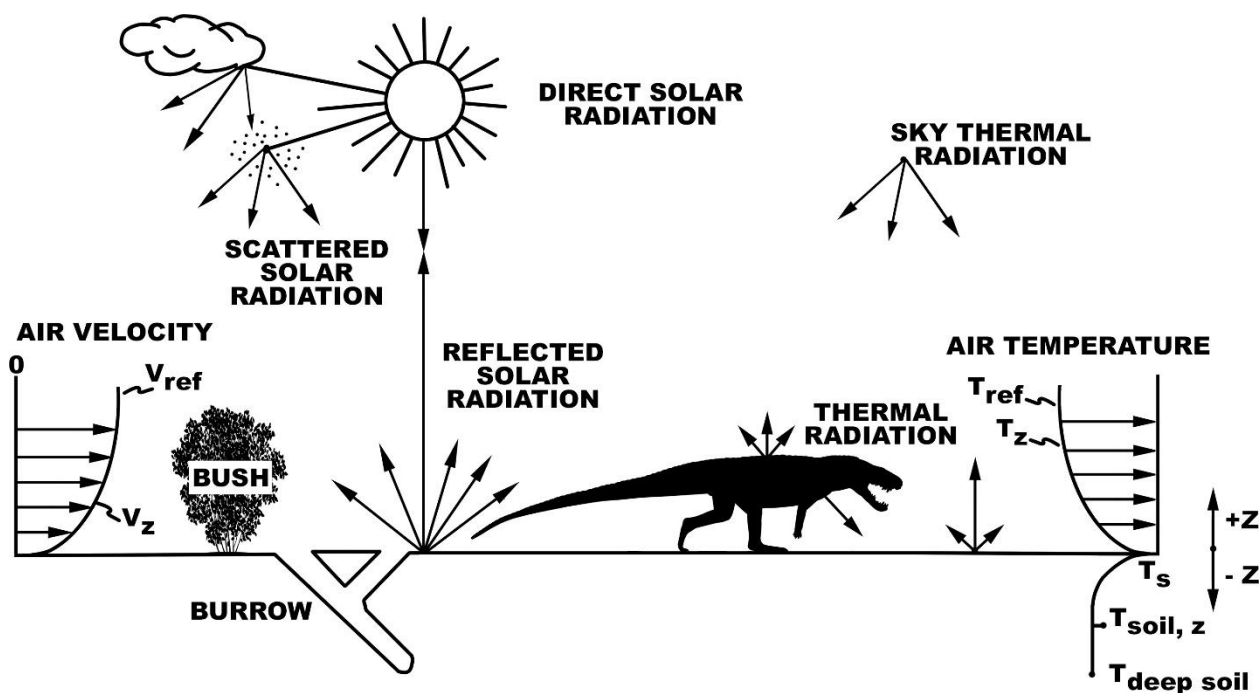


Figure 1. Organism–environment heat balance interactions. An organism’s heat balance that influences body temperature is determined by its microclimate conditions. Niche Mapper calculates microclimate conditions ranging from full sun to full shade, allowing an animal to seek a microclimate each hour where it can remain active, or not, if necessary, to optimize body temperature, energy demands and/or water balance.

Microclimate models were derived from the baseline Late Triassic microclimate model of Lovelace et al. [14], with individual models specified for a seasonally wet “monsoon” climate [34–36] and a more arid “desert” climate to simulate continental interiors at 12° latitude. To expand the range of geographic testing, a higher latitude (50°) microclimate based on Landwehrs et al. [37] was also run (Table 1). This is consistent with other findings that support a warm, dry climate for Late Triassic strata near 40–45° paleolatitudes in the northern and southern hemispheres (e.g., Greenland and Argentina/Brazil, respectively; [38–40]). We note that our high latitude model is more reflective of conditions on the western margin of Laurasia at ca. 45–50° where westerly winds bring warmer air masses from the south during winter months [36,38], and those of the southern hemisphere high latitudes (e.g., the fossiliferous Late Triassic Ischigualasto and Paraná basins of Gondwana).

Unlike the relatively consistent, latitudinally controlled temperature gradient in the southern hemisphere in winter months [36,38–40], the northern hemisphere experiences higher temperature variance in central and eastern high-latitude Laurasia, that may include periodic sub-zero temperatures [37,41] and paleofloral zonation [39]. These are beyond the scope of our current project, and are not reflected in this high latitude microclimate model.

Table 1. Maximum range of inputs for Late Triassic microclimate models. Ab-breviations: LowLat = Low Latitude, HiLat = High Latitude. See Tables S1 and S2 for seasonal variation.

Parameter	Model	Source	Input Range
Air Temperature	Microclimate	[14,36]	21–31 °C LowLat; 14–24 °C HiLat
Relative Humidity	Microclimate	[14,36,42]	Dry: 13–65%; Monsoon: 48–96%
Cloud Cover	Microclimate	[14,36]	50–90%
Wind Speeds	Microclimate	[14,43,44]	1–4 m/s
Atmospheric % O ₂	Biophysical	[14,45]	18%
Atmospheric % CO ₂	Biophysical	[14,46,47]	0.13%

2.2. Biophysical Models

Morphological measurements obtained directly from specimens and/or published data (see Supplemental File S1) were converted in Niche Mapper into simplified geometric shapes (e.g., cylinders, spheres, truncated cones, and ellipsoids) to represent the head, neck, limbs, torso, and tail (Figure 2). The simplified organismal model made up of geometric subunits allow core-to-surface temperature gradients to be computed for each body part [34,35]. In addition to the heat generated within each model subunit, user inputs can specify two insulatory layers: (1) presence or absence of a subcutaneous fat layer of a specified thickness; (2) presence and characteristics of epidermal insulation such as fur or feathers. Heat generated within the body must pass through either or both insulation layers (as specified) before being shed into the environment via radiation, convection and cutaneous evaporation.

Behavior can modify morphology and heat transfer pathways. Animals can be specified to adopt specific postures, such as laying down or sitting, in which case direct heat conductance to or from the ground can also be included in the heat balance calculation. Supplied with environmental conditions detailed in the microclimate model, Niche Mapper solves a heat balance equation for each hour of a model day, calculating heat lost to the environment via radiation (Q_{rad}), convection (Q_{conv}), cutaneous evaporation (Q_{evap}) and respiration (Q_{resp}), plus heat gained from the environment from direct and reflected solar input (Q_{sol}), heat generated internally (Q_{met}), and the amount of heat that can be transiently stored within the flesh (Q_{st}). This is calculated as follows:

$$Q_{met} - Q_{resp} - Q_{st} - Q_{evap} = Q_{rad} + Q_{conv} - Q_{sol} \quad (1)$$

If the animal is modeled as possessing an epidermal covering of fur or feathers, the additional layer slowing down heat transfer is accounted for by (Q_{fur}):

$$Q_{met} - Q_{resp} - Q_{st} - Q_{evap} = Q_{fur} = Q_{rad} + Q_{conv} - Q_{sol} \quad (2)$$

Body mass was calculated from body part volumes and assigned densities. Calculated total mass was checked against Graphic Double Integration and previously published mass estimates [48–50]. Diet composition was inferred from dental morphology [51,52]. Skin transpiration and breathing efficiency were estimated from extant analogs. For more detailed explanations of heat exchange across fur or feathers see [5,34,53].

Niche Mapper solves the heat and mass balance equation for individual body parts every hour of every day, which are then summed to provide the total metabolic rate necessary to maintain an organism's specified target core temperature. If the model is unable to maintain the target core temperature range within its allowed active metabolic rate within a given hour it will attempt to regain homeostasis by triggering a series of physiological and then behavioral modifiers to gain or shed heat as necessary.

Physiological solutions (when enabled) occur in the following order: (1) Increase fur or feather layer depth to increase insulation, similar to the piloerect response in extant mammals [54] and fluffing feathers in extant birds [6]; (2) Increase or decrease thermal conductivity of the outer "flesh" layer (to simulate vasodilation and vasoconstriction of

peripheral blood vessels); (3) Allow core body temperature to rise or fall (simulating temporary toleration of heat storage or loss) within a user defined range (see Modeled Late Triassic Taxa section below); (4) Increase the rate of surface evaporation (to simulate heat loss via sweating); (5) Increase respiratory heat loss (to simulate panting).

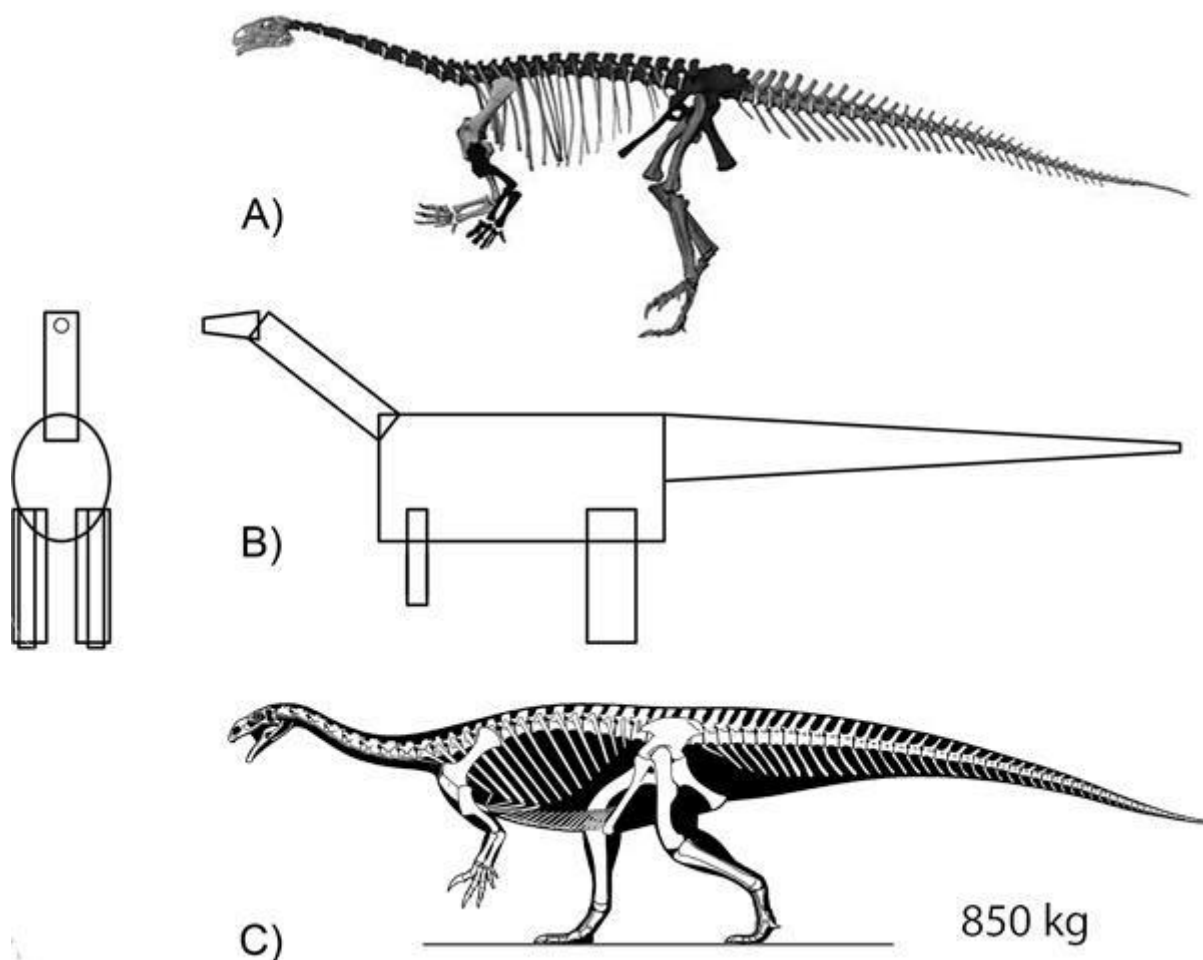


Figure 2. Creating proportional models for biophysical input. Linear dimensions are taken from fossil data (A), e.g., this surface scan of GPIT1. That data can be input to create a geometrically simplified (B) Niche Mapper model. A rigorous reconstruction of the skeletal anatomy can also be used to solve anatomical problems in 3D data (C) or to create silhouettes used to make independent GDI mass estimates.

If user-allowed physiological changes fail to maintain thermal homeostasis, user-enabled behavioral options are then triggered, including shade seeking, climbing, entering a burrow, wading, swimming, or adopting postures that reduce surface area in order to minimize heat loss (e.g., curling up). The heat balance equation is re-solved after each incremental thermoregulatory attempt until either the balance can be satisfied at that hour's metabolic rate (i.e., active or resting metabolic rate) or all thermoregulatory options are exhausted. In the latter case the thermoregulatory solution closest to the target metabolic rate is adopted for the hour—so excessive time spent at a local maxima or minima is an indication of lethal thermal stress.

Hourly energy consumption and water loss are integrated for the day, allowing for a mass balance equation to be calculated to establish daily food, water, and oxygen budgets. Q_{met} defines the necessary daily energy budget, which when adjusted for user-inputted caloric density of available food and digestive efficiency of the organism determines the food budget. Q_{met} also specifies the respiratory budget. Metabolic energy is directly tied

to oxygen consumption [55,56], and with user specified values for atmospheric oxygen percentage and the efficiency of extraction in the respiratory system the volumetric air flow through the respiratory system can be calculated.

For a detailed overview of all inputs for the biophysical model see Supplemental File S1 and [14]. When modeling extant organisms, the requisite physiological values can be measured directly or taken from values reported in the literature. With extinct species these values must be inferred, but the majority of inputs are either constrained by the physical properties of materials (e.g., fur, feathers, flesh conductivity) that are unlikely to have varied in the past, are relatively straightforward to infer from fossils (e.g., herbivory, carnivory, or omnivory), or turn out to have a minimal impact on modeled results (e.g., skin reflectivity and respiratory efficiency [14]). Some inputs such as digestive efficiency impact food budget but are not implicated in heat balance calculations [14]. Some behavioral responses were ruled out by size or gross anatomy (e.g., 500+ kg archosaurs are unlikely to have climbed trees or burrowed to avoid heat).

Other biophysical model inputs have a large influence on results and require more detailed inference. These include basal metabolic rate, target core body temperature, the presence or absence of epidermal insulation and the presence or absence of subcutaneous fat deposits. These are addressed by clade or genus as appropriate, along with the rationale for taxa selection in the following section.

2.3. Modeled Late Triassic Taxa

Representative terrestrial amniote taxa were selected covering four orders of magnitude in estimated mass from the Norian epoch of the Late Triassic period (Figure 3). In addition to taxonomic and mass diversity, our goal was to select taxa filling different ecological niches and a variety of metabolic and thermoregulatory strategies. In the following sections we explain the user-selected metabolic inputs modeled for each clade, and the data used to support those inferences.

2.3.1. Synapsids

The clade made up of mammals and stem-mammals is represented in this study by a dicynodont and a generalized basal mammalian morph. Dicynodonts were a group of herbivorous therapsids that were geographically widespread and diverse in the Late Permian and Early Triassic but steadily declined in diversity during the Middle and Late Triassic. By the Norian, remaining dicynodonts were restricted to a handful of large species [57].

While molecular clocks suggest an origin of crown-mammals in the Middle or early Late Triassic [58], to date the Late Triassic fossil record consists of the closely-related non-mammalian mammalian morph clades like *Tritylodonta*, *Docodonta* and *Morganucodonta* [59]. These mammal-like clades were small-bodied and likely insulated with fur [60].

Placerias—*Placerias* was a large (~800 kg) Late Triassic dicynodont that lived in North America (Lucas, 2002). Proportional measurements were taken from a cast of a large specimen on display at the New Mexico Museum of Natural History, which is based on specimens from the type quarry [61]. Given the widespread use of subcutaneous adipose tissue in extant mammals regardless of habitat [62], an adipose layer was modeled in Niche Mapper. Dicynodonts exhibit elevated rates of growth [63] and oxygen isotopes indicating a higher degree of endothermy than found in more basal tetrapods occurring in the same habitat [64]. However, coprolites assigned to a large Late Triassic dicynodont in Poland suggest a relatively simple digestive tract with long gut retention time, consistent with lower metabolic rates [65]. Together with the phylogenetic position of dicynodonts this suggests an incipient level of endothermy, perhaps on par with extant basal mammals such as monotremes. Based on this a target core temperature of 32 °C was used, and a monotreme-level BMR was calculated for use in the biophysical model based on [66].

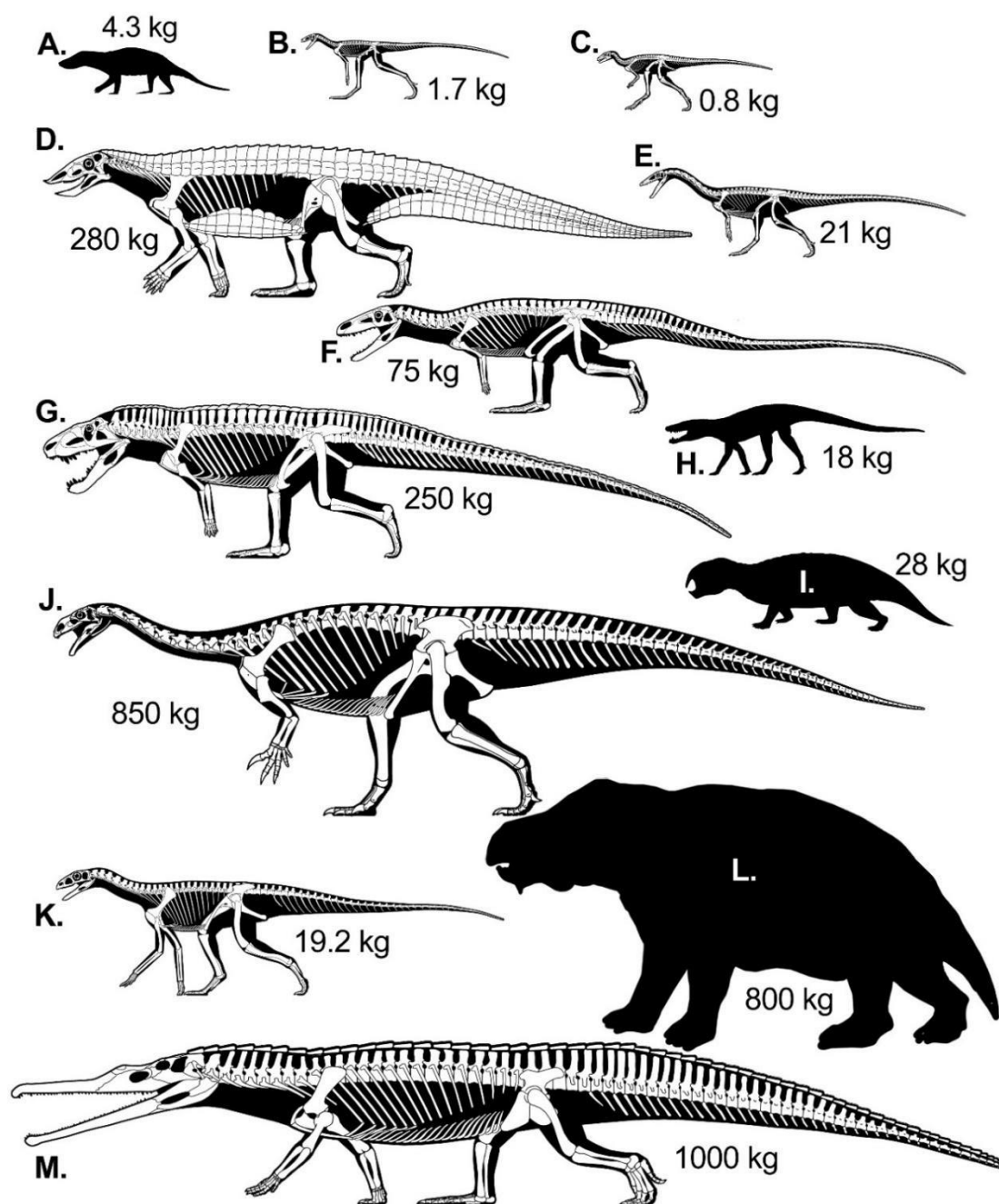


Figure 3. Representative skeletal and/or silhouettes with mass estimates of taxa used in this study. (A) Mammaliomorph (cf. *Tritylodon*), (B) *Dromomeron*, (C) hypothetical small ornithischian (cf. *Eocursor*), (D) *Desmatosuchus* (based on the skeleton of *Stegonolepis*), (E) *Coelophysis*, (F) *Poposaurus*, (G) *Postosuchus*, (H) *Hesperosuchus*, (I) rhynchosaur (cf. *Hyperodapedon*), (J) *Plateosaurus*, (K) silesaurid (cf. *Eucoelophysis*), (L) *Placerias* and (M) *Rutiodon*. Silhouettes A, I & H are modified Public Domain images from Phylopic.org (A & I), and Wikimedia Commons. L. provided by David Lovelace, all others are copyright Scott Hartman. Silhouettes are only loosely to scale, to provide visibility for smaller taxa. Rigorous skeletal reconstructions were made to help clarify proportional data, black silhouettes are schematic representations of taxa where proportional data was derived from literature or mount data.

The final variable to consider is the potential for fur-like epidermal structures. Fur-like structures were described in carnivorous coprolites from the Permian [67]. Since bones from dicynodonts were also common in the coprolites it was inferred that the

fur could potentially be linked to them. Given that other, more crownward synapsids were also potential prey in the Permian, it is unclear how strong this association is. The lack of more direct evidence is less problematic for *Placerias*, as similarly sized extant mammals (e.g., bison or small rhinoceros) in similar habitats (e.g., hippopotamus) suggest fur would be strongly reduced or absent, even if epidermal insulation was plesiomorphic in smaller, more basal dicynodonts. As such the skin was modeled without a fur layer, with evaporative cooling rates similar to extant naked-skinned mammals.

Mammaliamorph (cf. *Tritylodon*)—Mammaliaomorpha is defined as the most recent common ancestor of tritylodonts and mammals [68]. While ghost lineage and molecular clock data suggest that more derived mammaliaforms were a common part of Late Triassic ecosystems [58,69], Late Triassic mammaliaform body fossils are currently restricted to a single, controversially assigned tooth [70]. Tritylodont mammaliamorphs are better represented in Late Triassic sediments [71], achieved global distribution [71–73], and since they survived the End Triassic Extinction alongside their mammaliaform relatives, tritylodonts are a fruitful clade for future Mesozoic thermal ecology research [74]. Mammaliamorph inner-ear mechanics suggest endothermy was plesiomorphic to the group [75], although investigations into basal mammaliaform growth rates and femoral blood flow suggest this may have been a more incipient form of endothermy [76]. Given this signal we have elected to use a monotreme BMR estimate [66] and a similar (32 °C) target core temperature. Given the small size and similar ability in extant ecomorphs, the modeled animal was also allowed to seek shelter in burrows for thermoregulation. Direct evidence for epidermal insulation is first found within mammaliamorphs [60], but given their small size and at least incipient endothermy we utilized a mammal-like fur layer in the biophysical model, as well as skin evaporation values similar to extant mammals. Tritylodont tooth morphology has traditionally been inferred to indicate herbivory [77], although at least one tritylodont has been described as omnivorous [78] and extant mammals with similar tooth morphologies are also frequently omnivorous [79] and we have elected to model our general mammaliamorph similarly.

2.3.2. Archosaurormorpha

Archosauromorphs represent a large and diverse clade that includes all diapsids closer to birds and crocodiles than to lizards [80]. In addition to the more familiar derived archosaurs (a clade composed of the common ancestor of birds and crocodiles and all its descendants) basal archosauromorphs were represented in the Triassic by a diverse range of clades including those that adopted sprawling or upright gaits, occupied aquatic, arboreal and terrestrial habitats, and utilized herbivory as well as carnivory [80]. Basal archosauromorphs were diverse throughout most the Triassic but became more rare components of terrestrial ecosystems in the Late Triassic. They are represented in this study only by the beaked herbivorous rhynchosaurs, which survived until the mid-Late Triassic [80].

Rhynchosaur (cf. *Hyperodapedon*)—While rhynchosaurs died out before the end of the Carnian, they were an important component of Carnian ecosystems and so were included in this study. Niche Mapper proportions were based on the well-known *Hyperodapedon* [81]. Rhynchosaur osteohistology generally exhibits low, squamate-like growth rates [82,83] but does occasionally show elevated growth rates early in ontogeny [84]. Given their phylogenetic position, low growth rates, and lack of locomotory, respiratory, or food processing adaptations associated with higher basal metabolic rates, the rhynchosaur biophysical model was inputted with a squamate BMR, and a 30 °C target core temperature.

With no evidence of epidermal insulation outside of Archosauria, the rhynchosaur model used literature values for scaly skin dermal reflectivity and heat transmission [14]. Substantial subcutaneous fat layers are not widespread outside of synapsids [62], so a minimal adipose layer value was input for the rhynchosaur model. Allowing burrowing behavior in Niche Mapper is plausible; while a 28 kg animal would require a relatively large burrow, burrowing lizards exist at similar sizes [85]. Komodo dragon burrows have

been found for individuals that reach up to 70 kg [86]. Moreover, burrowing is widespread among sprawling, ectothermic species when thermally stressed [87].

2.3.3. Croc-Line Archosaurs

Pseudosuchians are archosaurs more closely related to crocodiles than to birds [88], and Middle and Late Triassic ecosystems were filled with a diverse array of pseudosuchian species. To capture a representative sample of their Triassic diversity, five pseudosuchian taxa were modeled.

Rutiodon—Although phytosaurs like *Rutiodon* superficially resemble living crocodilians (Figure 3M) they are distant relatives, being recovered as either the most primitive members of Pseudosuchia [80,89] or sometimes recovered outside of Archosauria altogether [88]. The skull and teeth of phytosaur suggest a similar ecological role to modern crocodilians, one based largely around fish and supplemented by the occasional terrestrial vertebrate. Despite their superficial similarity, trackways attributed to phytosaurs suggest they used a more upright stance, akin to the “high walk” that modern eusuchians only use on occasion [90]. Bone histology exhibits a growth pattern similar to living eusuchians [91,92], so an ectothermic BMR and a target core temperature of 30 °C was used in Niche Mapper.

Rutiodon is well known from several complete specimens, reaching lengths of up to 8 m, and a mass of 1000 kg [93,94]. Crocodile-like osteoderms are found in phytosaurs, so skin was modeled after extant eusuchian skin reflective properties, with no epidermal insulation and minimal subcutaneous fat insulation.

Desmatosuchus—Aetosaurs were heavily armored, herbivorous pseudosuchians found only in the Late Triassic [95]. Histologically determined growth rates generally match those of phytosaurs and extant eusuchians [91,92]. Modern crocodilian values were therefore used for skin, insulation, BMR, target core temperature (30 °C) and evaporative cooling inputs, similar to *Rutiodon*. *Desmatosuchus* grew up to 4.5 m in length and perhaps 300 kg [96]. Some anatomical proportions were filled in from better described remains of other aetosaurs (Figure 3D; e.g., [97]).

Poposaurus—The eponymous species in Poposauridae, a more crownward clade of carnivorous Late Triassic loricatan pseudosuchians [88]. Despite being a croc-line archosaur that is closer to extant crocodilians than phytosaurs and aetosaurs, poposaurids were obligate bipeds, converging on the condition seen in theropod dinosaurs [98]. *Poposaurus* is known from a virtually complete and well-described postcranial specimen, YPM 57100 which formed the basis of the proportional inputs for the biophysical model (Figure 3F; [99]).

The expanded pelvic musculature suggests a shift to Type I, slow-twitch muscle fibers and increased scope in locomotion [99,100]. Histological analysis of *Poposaurus* shows a pattern of rapid growth more similar to dinosauriforms, but with bone vascularization levels overlapping the range of extant eusuchians [99]; smaller-bodied poposaurids show evidence of slower growth rates [101]. Although poposaurids show a reduction in dermal armor, there is no evidence for epidermal insulatory structures or other heat-retaining adaptations in the group. Taken as a whole, poposaurids show evidence of elevated metabolic activity compared to extant crocodilians, but below the level seen in dinosaurs. We used the lowest level endothermic BMR (“monotreme” [66]) and a target core temperature intermediate to that of extant ectotherms and endotherms (35 °C). Other dermal values were adopted from extant relatives [14].

Postosuchus—Moving further crownward, rauisuchids are a group of large, exclusively carnivorous loricatans from the Middle and Late Triassic. *Postosuchus* reached 4.5 m in length and an estimated mass of 250+ kg [102,103]. The type and paratype specimens of *Postosuchus* were used as the basis of the proportional inputs (Figure 3G; [103]). *Postosuchus* is also primarily bipedal, though given the number of quadrupedal intermediates between it and poposaurids it is clear this was another independent origin of bipedal locomotion in the Late Triassic [88,103]. *Postosuchus* appears less committed to obligate bipedalism than *Poposaurus*, in that the slightly built forelimbs could probably bear weight at low

speeds, and there appears to be an ontogenetic shift to shorter arms as individuals age (cf. specimens in [103]) suggesting the possibility of facultatively quadrupedal hatchling or juvenile stages.

Postosuchus likely had a similar BMR to *Poposaurus*. Histology shows an elevated rate of growth compared to modern crocodylians, but less so than seen in dinosauriforms or even the fastest growing loricatans [104,105]. BMR and target core temperature (35 °C) were the same as used as for *Poposaurus*. Osteoderms are known for *Postosuchus*, so it can be unambiguously assigned to a skin type similar to living crocodylians [103].

Hesperosuchus—Moving one final step crownward, crocodylomorphs are the loricatan clade that contains living crocodylians. Despite their phylogenetic proximity, Late Triassic crocodylomorphs were in many ways the least similar to living crocodylians in ecology and gross anatomy, consisting of small-to-medium sized gracile, terrestrial carnivores [88]. The upright, quadrupedal stance of basal Late Triassic crocodylomorphs like *Hesperosuchus* included limbs with cursorial proportions [106,107]. The Niche Mapper model body part proportions were taken primarily from AMNH 6758 [108].

Despite being the most cursorial pseudosuchian in the model dataset, *Hesperosuchus* bones exhibit degrees of vascularization and growth rates almost identical to that seen in living crocodylians [82]. While faster growth requires more energy and a concomitant increase in metabolic rate, the opposite is not necessarily true [109], with *Homo sapiens* being a notable example of an endothermic amniote with a slow growth rate [110]. Since the return to a secondarily reduced ectothermic BMR in living crocodylians has been tied to reinvading aquatic habitats [82,111,112], and *Hesperosuchus* shows no evidence of aquatic adaptations, incipient endothermic BMR levels and an intermediate target core temperature of 35 °C like other loricatans was used. The presence of unambiguous osteoderms in basal crocodylomorphs allows for the use of extant crocodylian literature values for skin reflectance and flesh conductivity [113].

2.3.4. Bird-Line Archosaurs

Ornithodirans are the clade made up of the most recent common ancestor of birds (dinosauriforms) and pterosaurs (pterosauromorphs), and all its descendants [114]. Ichthyological data suggests an Early Triassic origin for dinosauriforms [115], and by extension presumably pterosauromorphs, although body fossils do not show up until the Middle and Late Triassic, respectively. Lagerpetids were traditionally considered dinosauriforms, but recent phylogenetic work has recovered them as basal pterosauromorphs [116]. While the basal dinosauriform *Marasuchus* and several lagerpetids were quite small at under a meter in length [116,117], dinosauriform silesaurs and some pterosauromorphs grew to two meters or more [118], and by the end of the Triassic prosauropod dinosaurs had reached a ton or more in mass [119]. To capture this variability in size, ecology and phylogeny, we have selected a small lagerpetid (*Dromomeron*) and medium-sized silesaurid as our non-dinosaur ornithodiran taxa. Due to converging lines of evidence that include growth rates, isotope paleothermometry, and anatomical indicators of enhanced aerobic scope all ornithodirans appear to have been at least incipiently endothermic [120–122].

Dromomeron—A basal lagerpetid pterosauromorph, *Dromomeron* was an ~1 m long, bipedal omnivore of the Late Triassic [123,124]. *Dromomeron* is mostly known from hind limb elements, so other lagerpetids contributed to a composite reconstruction (Figure 3B) to achieve proportional inputs [117,125]. Histological analysis of the femur of *Dromomeron* demonstrates an elevated growth rate similar to those seen in croc-line archosaurs showing incipient endothermy [82,124], so a similar BMR and target core temperature (35 °C) were assigned.

The presence or absence of epidermal insulation in basal dinosauriforms and pterosauromorphs is more contentious. There is extensive evidence for epidermal coverings in pterosaurs [126–128], small-medium sized theropods [129–131] and some small ornithischian dinosaurs [132,133] as far back as the Early Jurassic [134]. Detailed morphological similarity to epidermal structures in pterosaurs has been used to argue that some form of

epidermal insulation is primitive to all ornithodirans [135]. However, while all pterosaurs were likely covered in epidermal insulator structures [127], many large dinosaur clades only exhibit reticulate scales and/or osteoderms, and in the absence of direct evidence Triassic taxa character optimization studies do not always favor epidermal filaments pleiomorphic to Ornithodira [136]. Despite opposition to fully homologous filaments across Ornithodira, Campione et al. postulate a scenario wherein similar genes are co-opted repeatedly in ornithodirans of small size. This opposition to basal epidermal insulation is also problematic, as the absence of direct, physical epidermal data at the base of Ornithodira and the resulting limited species which can confidently be assigned character states to optimize, risks systematic bias in the results [137,138]. Given *Dromomeron's* small size (1.7 kg) the biophysical input model was specified with a reduced, incipient layer of epidermal filaments.

Finally, with lagerpetids reinterpreted as basal pterosauromorphs [116] and more complete skeletal remains being described [125], there has also been a functional shift from interpreting lagerpetids as strictly terrestrial to cursorial, or potentially even arboreal habitats. That said, since broadly similar clades often contain both terrestrial, scansorial and arboreal members (e.g., Sciuridae [139]), since taking shelter inside a tree or other structure serves broadly the same use as burrowing [140], and to make this model broadly applicable to small dinosauromorphs as well as pterosauromorphs, we have enabled the “burrow” flag in Niche Mapper to allow the model to seek thermal shelter.

Silesaurid (cf. *Eucoelophysis*)—Silesaurids were a group of omnivorous or insectivorous, generally small (1–3 m length), facultatively quadrupedal dinosauromorphs usually recovered as the sister group to Dinosauria [141,142]. Silesaurids were a common part of Middle Triassic and Late Triassic ecosystems [141,143]. Late Triassic silesaurid remains are largely incomplete, so the Middle Triassic *Asilisaurus* was scaled to the appropriate size to provide proportional data (Figure 3K). Silesaurid histology exhibits growth rates and bone texture intermediate between *Dromomeron* and early dinosaurs [124], so an incipient endothermic BMR was assigned along with a target core temperature of 37 °C, intermediate between *Dromomeron* and dinosaurs.

Small ornithischian (cf. *Eocursor*)—Substantial taxonomic revision of fragmentary specimens eliminated nearly all putative ornithischians from the Triassic [144,145]. One possible exception is *Eocursor*, is clearly an ornithischian [146] but its Late Triassic/Early Jurassic status depends on stratigraphic resolution within the Elliot Formation [147]. Regardless, ghost lineages suggest the presence of small ornithischians by the Late Triassic, so modeling a representative taxon is informative about the clade’s ability to inhabit Late Triassic ecosystems.

Within Dinosauria, more derived endothermy is supported by multiple lines of evidence including circulatory pressure [148], isotope paleothermometry [121], osteological correlates for increased respiratory performance [149], power generation during locomotion [120,150] and the majority of dinosaurian growth rates [109]. A ratite level of BMR was calculated [151], and a target core temperature of 38 °C was used [14,152]. Jurassic small-bodied ornithischians with evidence for dermal impressions show several types of filamentous structures [132,133], so an epidermal insulatory layer was modeled. Taphonomy supports burrowing in small ornithischian taxa [153].

Plateosaurus—Basal sauropodomorphs appeared in the Late Triassic as small, omnivorous bipeds [154], but by the end of the Late Triassic they were medium to large sized bipedal herbivores, with some reaching a tonne or more in mass [119,155]. Proportional data was taken from GPIT1 (Figures 2 and 3); [119]). In addition to arguments supporting an elevated metabolism made above for all dinosaurs, [14] we modeled and tested *Plateosaurus* in a Niche Mapper virtual metabolic chamber and concluded that a ratite-like BMR was the most plausible condition, so a 38 °C target core temperature and a ratite-level BMR was used. Other biophysical inputs were adopted from the same vetted model [14].

Coelophysis—Theropod dinosaurs are the clade that includes birds. Body fossils are first found in the Late Triassic, and by the end of the Triassic theropod-bearing ecosystems

are dominated by coelophysids [156]. While no direct evidence is present for or against epidermal filaments, they are so far ubiquitous in small theropods preserved with skin impressions. As with *Plateosaurus*, *Coelophysis* was extensively modeled and vetted in Niche Mapper previously [14], from which all biophysical input values were adopted, including a ratite-level BMR and a target core temperature of 38 °C.

2.4. Niche Mapper Plots

Niche Mapper output files were collated in R [21] and converted into plots using ggplot2 [24]. After solving heat and mass balance equations allowing the 13 model organisms to thermoregulate within a specified microclimate model for a year, Niche Mapper outputs hourly values for each taxa in each of the four microclimates producing 15,600 output values in each of 64 different categories ($n = 998,400$ data points). Seasonal and daily thermal performance visualization allows for interpretation of times of heat stress in context, which we achieved by plotting each organism's core body temperature (T_{core}), metabolic energy use (ME), and percent hourly shade seeking behavior necessary to thermoregulate within a microenvironment (cf. [14]; all raw data is available in Supplemental Database S5).

Figure 4 shows two representative T_{core} plots for a 280 kg *Desmotosuchus* in wet ('Monsoon', Figure 4A) and arid ('Desert', Figure 4B) microclimate models. The microclimate models are derived from geochemical proxies representative of low-latitude Late Triassic environments in North America [14,157]. Examining both plots at mid-September, in the monsoon microclimate *Desmotosuchus* was able to maintain its T_{core} within a ± 3 °C range of its target core temperature value for most of the day, where enzymatic processes are operating at their maximal efficiency [158]. In the desert microclimate on the same day of the model year the *Desmotosuchus* experienced thermal stress for 8 h at midday, with its core body temperature entering the range where structural changes would reduce enzymatic efficiency, and at higher temperatures eventually risk denaturing of enzyme proteins [159].

Looking at metabolic energy, in the low-latitude monsoon microclimate the 280 kg *Desmotosuchus* can be active all day (Figure 5A), albeit with increased metabolic rates from ~2 times BMR to 3–4 times BMR in morning and evening hours. This results in an increase in daily energy expenditure (DEE), which is presumably non-optimal, but research shows DEE is only tightly linked to BMR in placental mammals [160,161], and with sufficient foraging time ME increases are not inherently a problem until extreme multiples (5× or more) of BMR become necessary [14]. In the arid microclimate (Figure 5B), for 4 h at midday there is significant heat buildup, which cannot easily be offset by metabolic changes as an organism cannot reduce ME below the basic metabolic processes necessary to keep the animal alive (i.e., BMR), and when active, ME cannot be reduced even that far. So in the arid environment between the months of April and October a 280 kg *Desmotosuchus* would have encountered elevated temperatures when foraging at midday, and would presumably have altered its foraging time to avoid dangerous heat buildup (cf. [162]), which is common in modern desert ectotherms.

Shade seeking behavior is an energetically inexpensive way to thermoregulate. Shade seeking may occur during daylight hours when T_{core} is too high to reduce incoming solar radiation and to shelter in a cooler microenvironment. Shade seeking can also occur at night to maintain heat, as vegetative cover slows radiant heat loss by exchanging heat with an overhead vegetative canopy rather than a much cooler clear night sky (Lovelace et al., 2020). In the monsoon microenvironment the modeled *Desmotosuchus* seeks 'night shade' for warmth during overnight hours, but retains 15 h of foraging time without needing to seek shade (Figure 6A). In the arid microclimate, the same 280 kg *Desmotosuchus* would be forced to retreat to the shade for 7 h around midday, but also would need to seek night shade for a similar amount of time as in the monsoon microclimate, resulting in just 7 h a day of foraging unencumbered by the need to seek some form of cover (Figure 6B).

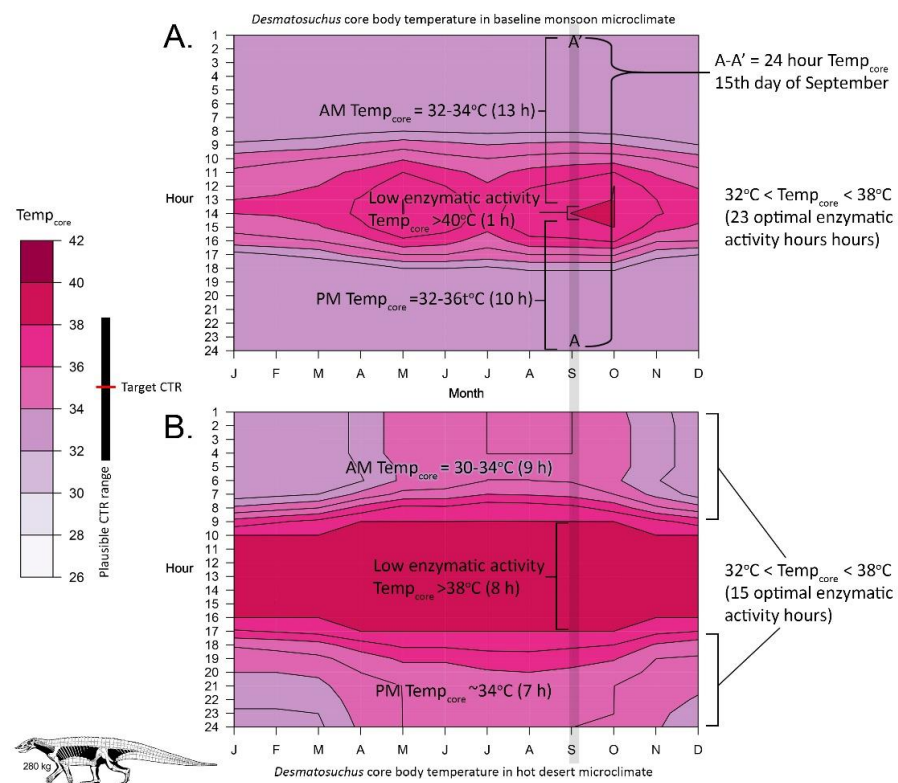


Figure 4. Daily fluctuations in core temperature, affecting enzymatic efficiency. Core body temperature plots delimiting active foraging hours for a 280 kg *Desmatosuchus* throughout a modeled year in (A) Low latitude Monsoon and (B) Low latitude arid microclimates.

The viability of herbivores with significant shade-seeking requirements depends on resource density within the environment, and the necessary foraging hours required to meet an organism's DEE. In a heavily forested area, seeking shade may not be a problem, but Late Triassic continental interiors were arid, and in wetter areas megamonsoon conditions seasonal aridity kept stands of trees spaced out and restricted to year-round sources of water [163,164], so shade seeking behavior can quickly become a problem if it restricts foraging time to the point that it's no longer possible to reliably consume enough energy to meet DEE, which for large herbivores can be 50–70% of each day [165,166].

2.5. Interpreting Burrowing Results

For taxa that we allowed to burrow, such as *Dromomeron*, a heuristic challenge with interpreting plots arises (Figure 7). Since burrows insulate occupants from the external environment, the metabolic costs of thermoregulation drop to near-BMRs levels while they are inside. While the ME plots show this accurately, an unintended consequence is that time spent in a burrow—the easiest and safest thermoregulation available—appears identical to the lowered ME seen in non-burrowing taxa as an attempt to avoid excess heat buildup, one of the most dangerous forms of heat stress (e.g., compare *Dromomeron* in Figure 7 to *Desmatosuchus* in Figure 5).

Our taxa with burrowing enabled (small ornithischian, *Dromomeron*, mammalianomorph, *Hesperosuchus*, and rhynchosaur) were run with and without burrowing enabled (plots for both can be found in Supplementary Files S4 and S5). Running simulations without burrowing is informative about the ability of small taxa to function outside their burrow (e.g., if forced to leave due to changing climatic conditions). For consistency in interpretation, we present whole-ecosystem aggregate microclimate results without burrowing enabled for any taxon, with follow-up figures presenting the thermal performance of taxa in which burrowing was enabled explicitly labeled as such. All ecosystem plots are ordered left to right and top to bottom from smallest taxa to largest.

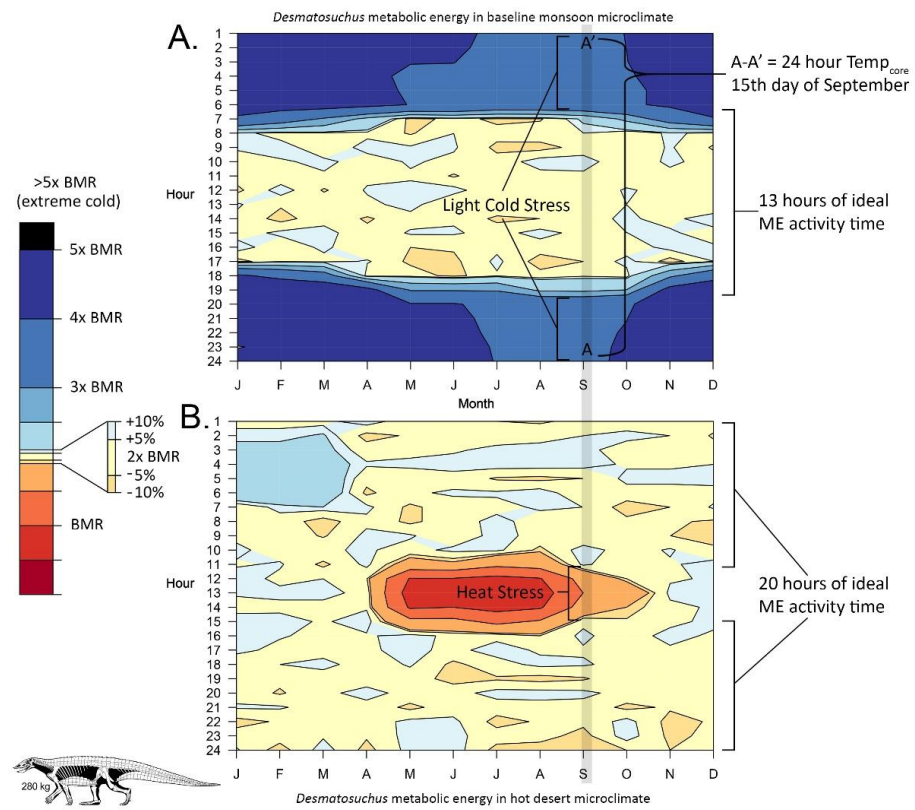


Figure 5. Daily fluctuations in metabolic energy. Metabolic energy plots for a 280 kg *Desmatosuchus* thermoregulating in low latitude monsoon (A) and low latitude arid (B) microclimates.

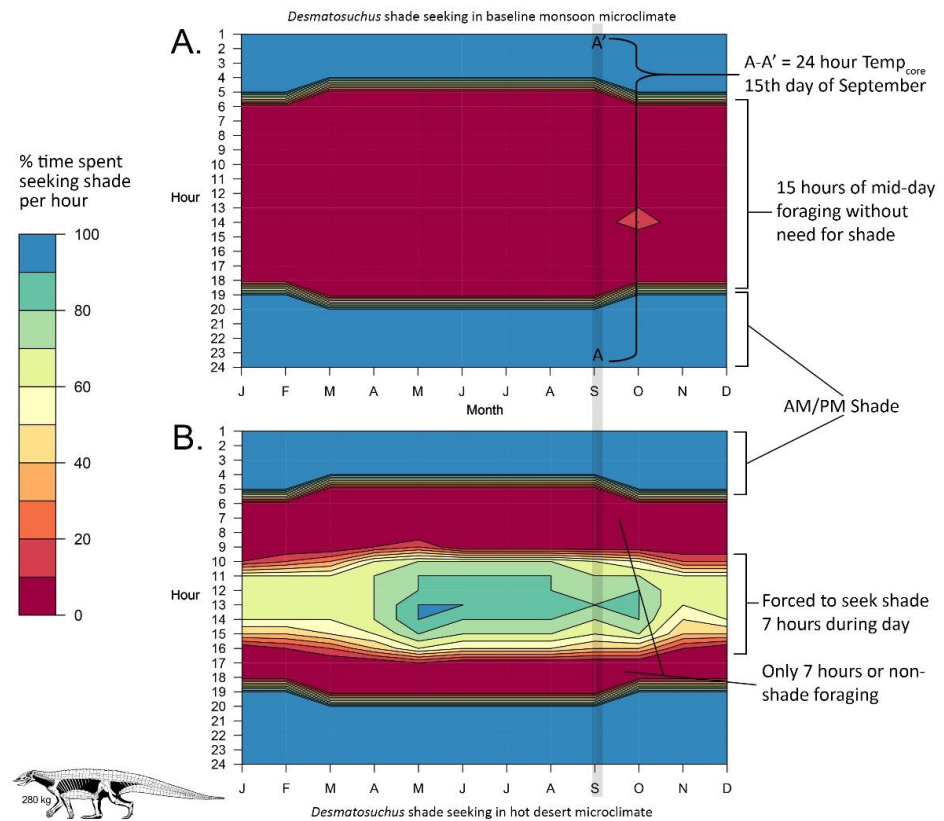


Figure 6. Daily fluctuations in shade seeking behavior. Modeled behavioral results for shade-seeking in a 280 kg *Desmatosuchus* in low latitude monsoon (A) and low latitude arid (B) microclimates.

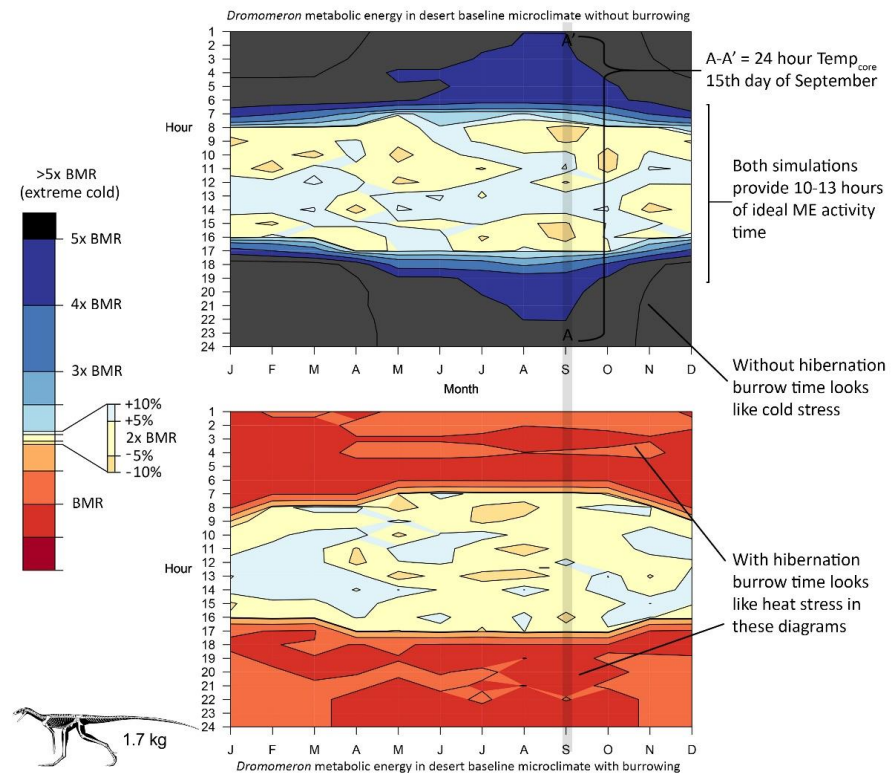


Figure 7. Impact of modeling torpor on ME plots. Daily fluctuations in shade seeking behavior by a 1.5 kg *Dromomeron* without ‘hibernation’ flagged (**top**) and with ‘hibernation’ enabled (**bottom**). Note this behavior is torpor, and not true mammalian hibernation.

Thermal Ecology of Baseline Monsoon Microclimate at Low Latitude

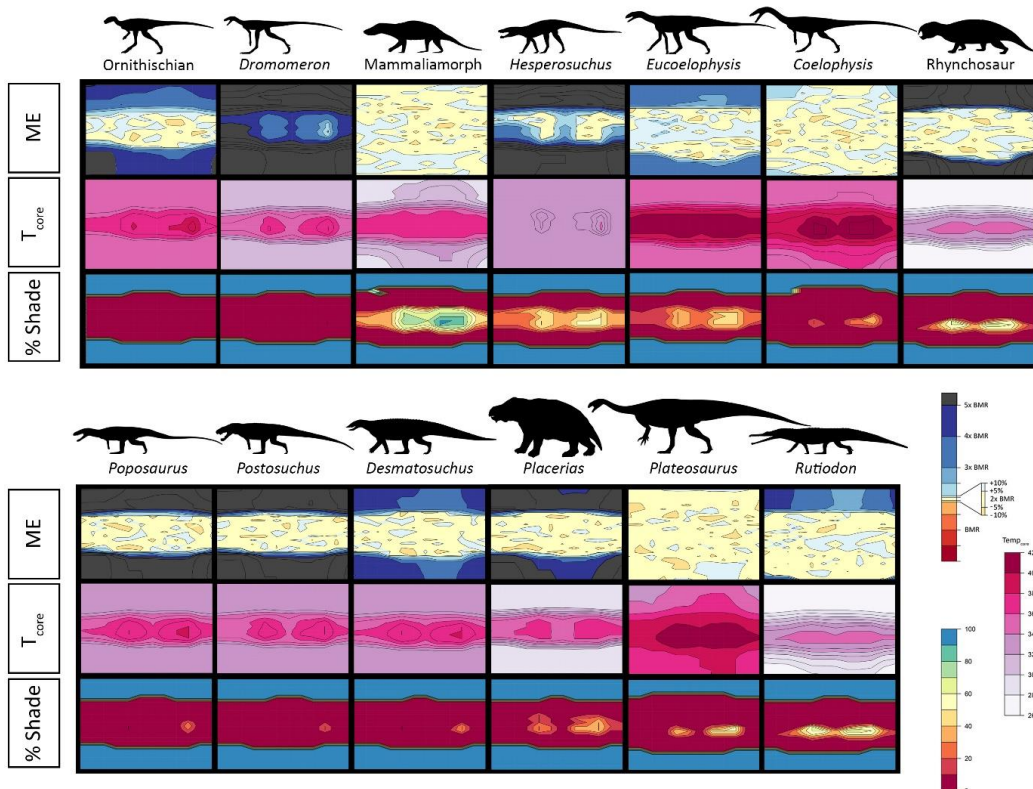


Figure 8. Thermal ecology in a typical Late Triassic seasonal monsoon environment at 12 degrees

latitude. Burrowing is not enabled. Species are arranged from smallest to largest, left to right and top to bottom. Full size color keys can be found in Figures 4–7. Abbreviations: ME, metabolic energy; T_{core} , core temperature; %Shade, amount of time per hour an animal must seek out shade to thermoregulate.

2.6. Results for Environmental Simulations

Three plots are produced for each of the 13 taxa in each of the 13 microclimate models, resulting in 156 full resolution plots. Since much of the value of the plots come from comparing results between taxa within the same microclimate, results are presented with reduced scale images of 39 plots each (e.g., Figure 8). Collated pdfs of individual full-resolution plots are available in Supplemental Files S1 and S2).

3. Results

Looking at the results of low latitude Late Triassic microclimates [14,37] there is little difference in thermal performance between the monsoon and arid environments (Figures 8–10). The arid environment shows a slight increase in shade seeking behavior at midday for most taxa, with *Placerias* the most impacted with a 1.5% increase in shade seeking behavior during a simulated year. Conversely, the small terrestrial crocodylian *Hesperosuchus* needs to seek 0.4% less shade in the more arid environment. The theropod *Coelophysis* needed to seek more midday shade in the monsoon microclimate but required less night shade for a net gain of 1.9% foraging time. Given daily variation in foraging efficiency, annual variations in climate and longer variations due to orbital forcing [167] it seems unlikely that these small changes to foraging time would have impacted survival. Indeed, with similar temperatures shared between the monsoon and arid microclimates thermal variation between them is too small to directly impact habitat preference; instead, non-thermal factors like water availability and food resource density would have been more important in habitat selection [168]. Based on sedimentological and geochemical proxies, seasonal monsoon conditions would have dominated low latitude portions of Pangea due to the Late Triassic mega-monsoon [169], but exceptionally arid, desert-like conditions were common in the continental interiors [164], see Discussion below.

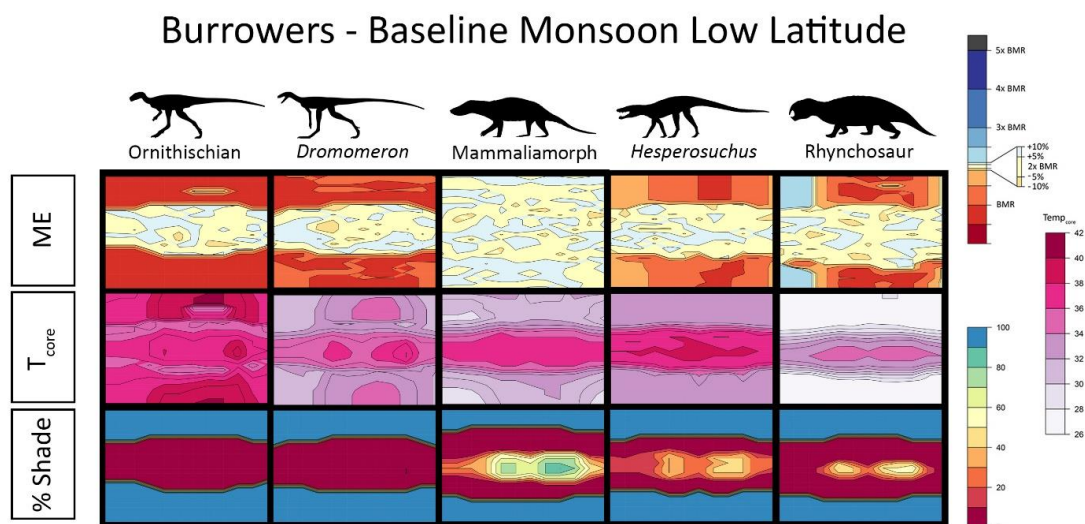


Figure 9. Thermal ecology with burrowing enabled in the baseline monsoon environment at 12 degrees latitude. Species are arranged from smallest to largest left to right. Red areas in the metabolic energy plots are due to lowered thermoregulation costs while in a burrow, not from heat stress. Full size color keys can be found in Figures 4–7. Abbreviations: ME, metabolic energy; T_{core} , core temperature; %Shade, amount of time per hour an animal must seek out shade to thermoregulate.

Thermal Ecology of Baseline Arid Microclimate at Low Latitude

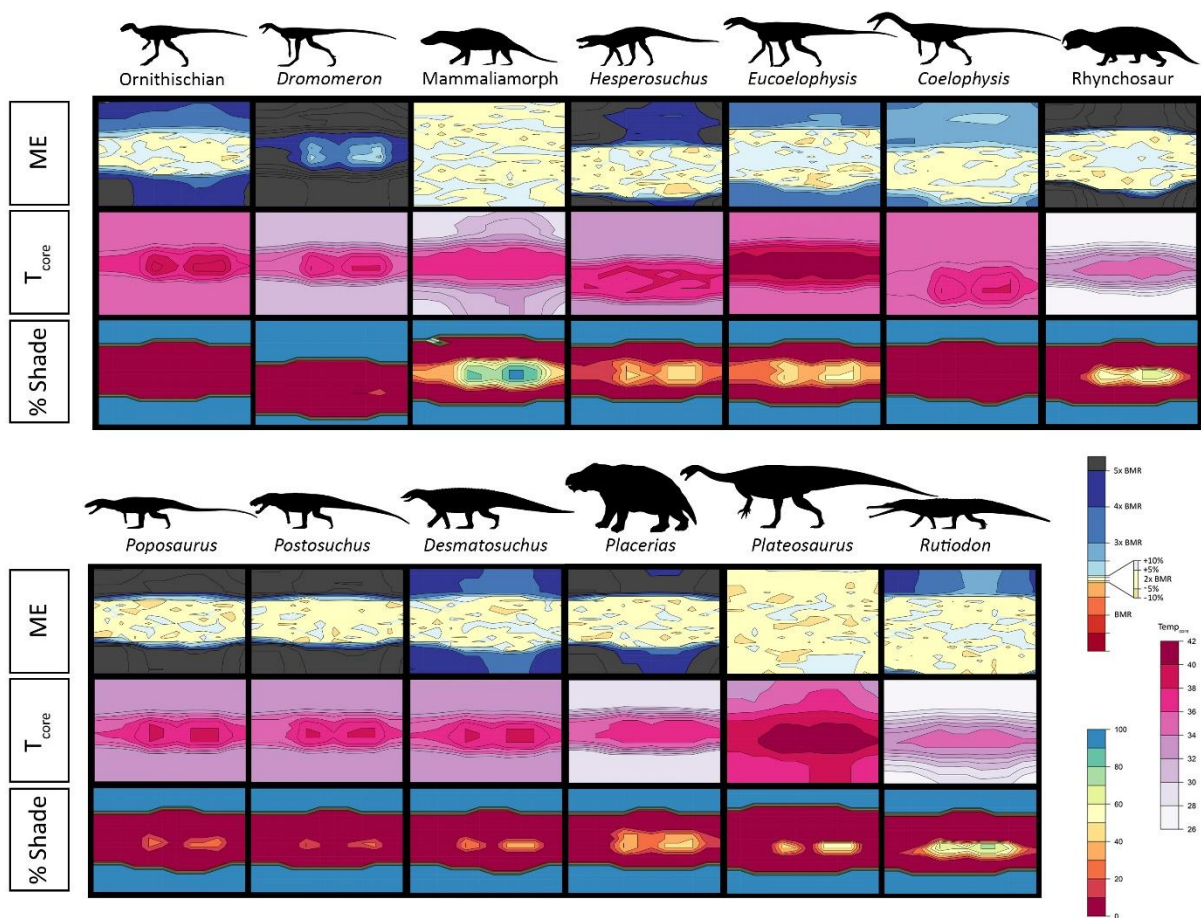


Figure 10. Thermal ecology in an arid, low latitude Late Triassic environment. Species are arranged from smallest to largest left to right and top to bottom. Full size color keys can be found in Figures 4–7. Abbreviations: ME, metabolic energy; T_{core} , core temperature; %Shade, amount of time per hour an animal must seek out shade to thermoregulate.

The modeled ornithischian was able to thermoregulate at night most of the year by raising its ME to 3–4.5 \times BMR, but enabling burrowing (Figure 9) resulted in a warmer T_{core} and lower ME overnight. Burrowing therefore seems probable but is not strictly necessary on thermal ecology grounds. In contrast, *Dromomeron* is non-viable without burrowing enabled (Figures 8 and 10). When allowed to use a burrow overnight (Figure 9) *Dromomeron* maintains an elevated T_{core} at little ME cost, and can use thermal inertia and potential trips back to the burrow as necessary to forage successfully throughout the day. Based on these results it appears *Dromomeron* was an obligate burrower/shelter seeker and almost certainly diurnal, whereas the small ornithischian could engage in crepuscular or cathemeral activity patterns without encountering strong thermal constraints, though the elevated ME costs at night outside the burrow suggest that being nocturnal was less likely.

The 4.3 kg mammaliomorph could thermoregulate at night year-round with or without burrowing enabled (Figures 8 and 9). Aside from being larger than either the small ornithischian or *Dromomeron*, the mammaliaform's denser mammal-based epidermal insulation and a reduced surface area to mass ratio owing to its more compact build account for these differences. During the day the mammaliomorph core temperature regularly rose above 36 $^{\circ}$ C (from a T_{core} of 32 $^{\circ}$ C), so foraging would have been more thermally favorable at night, especially since its small size (4.3 kg) would allow it to forage under foliage cover that provides night shade. This result is congruous with well-developed olfactory and acoustic

anatomy in mammalianomorphs, which have been interpreted as evidence for subterranean and nocturnal habitats being widespread within the clade [59].

The other burrowing taxa, *Hesperosuchus* and rhynchosaur, would have been immediately under significant cold stress if they left their dens at night in either modeled environment, year-round (Figures 8 and 10). With burrowing enabled (Figure 9) both taxa function effectively as diurnal animals, though the rhynchosaur would be forced to expend additional ME to warm itself even in a burrow during the winter months.

The 19.2 kg *Eucoelophysis* was not modeled as a burrower and maintained its core temperature overnight without excessive ME costs. At midday during much of the year T_{core} would rise above the target of 37 °C enough to result in shade seeking behavior. In summer months that could elevate to 40–42 °C, resulting not only in reduced foraging time but the potential for reduced enzymatic function and a risk of heat stroke for hours at a time. Given this pattern of thermal constraints and the insectivorous/omnivorous diets inferred for silesaurids [142], a crepuscular activity pattern would make the most sense in these environments.

The 21 kg theropod *Coelophysis* was able to thermoregulate at night with minimal ME expenditure (Figures 8 and 10), supporting the interpretation of it as a non-burrower. During the summer half of the year its T_{core} would rise from a targeted 38 °C to 42 °C, resulting in extensive shade seeking behavior. Despite the longstanding assumption that Mesozoic dinosaurs were largely diurnal (e.g., [170]), a nocturnal, crepuscular, or cathemeral sleep cycle all seem more likely. The closely-related Early Jurassic *Megapnosaurus rhodesiensis* from South Africa was previously found to be nocturnal based on sclerotic ring morphology [171], further reinforcing how unlikely a diurnal lifestyle was for Late Triassic *Coelophysis*.

The two bipedal pseudosuchians *Poposaurus* and *Postosuchus* are remarkably alike in the baseline conditions, despite the latter at 250 kg out-massing the former (75 kg). Both thermoregulate effectively during the day but face excessive cold stress at night. While traditionally not thought of as burrowing animals due to their size and lack of obvious digging adaptations, Komodo dragons (up to 70 kg) and American alligators (up to 450 kg) burrow, though it's not clear if there is a size limit to when individual alligators stop burrowing [86,172].

The armored, 280 kg *Desmotosuchus* performs better, maintaining a viable T_{core} without expending excessive amounts of ME. *Desmotosuchus* also avoids shade seeking behavior for all but a couple of hours a day during the hottest months of the year. The much larger but similarly low BMR pseudosuchian *Rutiodon* follows a similar pattern, although its larger thermal inertia allows it to stay warmer overnight (Figures 8 and 10).

The 800 kg herbivorous stem-mammal *Placerias* appears to experience an unfavorable combination of cold stress at night year-round, and up to 6 h daily of 20–40% shade seeking behavior at midday. It is possible that the current consensus view of dicynodonts is wrong, and they had more derived endothermy and/or better developed epidermal insulation. Alternatively, at least some dicynodonts have been inferred to be aquatic or semi-aquatic, like stem-mammalian hippos [173,174], and multiple species (including *Placerias*) have been found in social groupings in autochthonous quarries [61,175,176]. *Placerias* long bone histology is consistent with a semi-aquatic lifestyle [177], and the type quarry of *Placerias* [61] is a low-energy, high water table environment containing a multi-generational bone bed with a minimum of 40 individuals; there is no evidence of hydrologic transport or sorting [61]. Other dicynodonts have also been inferred to be social [175,178]. If *Placerias* were using standing water to cool off during summer days and grouping up as a herd to conserve heat at night it would solve the apparent paradox of these results. Huddling behavior has been modeled in Niche Mapper as a thermoregulatory strategy in vervet monkeys [179] and is a promising topic for future analyses of dicynodont thermoregulatory behavior.

The 850 kg herbivorous dinosaur *Plateosaurus* was able to thermoregulate at night with low ME expenditure, but encounters up to 9 h of daylight where its T_{core} is between

40 and 42 °C. While 40 °C is only 2° warmer than the *Plateosaurus* target T_{core} of 38 °C, once vertebrates pass 40 °C ME can quickly spiral out of control as cell membrane permeability starts to increase exponentially, requiring extensive active transport to maintain ion gradients necessary to mitochondrial function and homeostasis [180]. This means *Plateosaurus* would have regularly risked critical heat loading during summer months. It is tempting to ascribe a nocturnal activity cycle to *Plateosaurus*, but large herbivores are rarely nocturnal, and without the ability to burrow to reduce its midday heat load *Plateosaurus* would have become dangerously hot even while sleeping during the day. Indeed, the best solution would to simply be absent from these environments, and as noted by [14], *Plateosaurus* and other larger sauropodomorphs are absent from low latitude habitats in the Late Triassic.

Turning to higher latitude (55°) microclimate models, we see the impact of cooler temperatures [37] and stronger seasonality on modeled taxa (Figures 11–13), with colder winters that limit activity for some taxa. The amount of precipitation (Figures 11 and 12) makes an even smaller difference at high latitudes than it did in the low latitude microclimates. Without burrowing enabled, burrowing taxa except the mammalianomorph are non-viable, requiring too much ME year-round to maintain T_{core} . With burrowing enabled (Figure 13), the small ornithischian, *Dromomeron*, and *Hesperosuchus* maintain viable T_{core} year-round, albeit with very different foraging strategies. The ornithischian with its elevated BMR and epidermal insulation displays monotonic conditions across the modeled year, able to maintain ideal T_{core} at reduced ME levels, while spending up to 30% of each hour in its burrow. Being agnostic regarding daily thermal patterns suggests a cathemeral behavioral pattern, although any behavioral pattern would be plausible, allowing for behavioral flexibility to adapt to changing circumstances (including seasonal amounts of daylight, local weather patterns, etc.). *Dromomeron* was more constrained by the need to seek shade most of the year to thermoregulate (Figure 13). Foraging in shade would be consistent with an arboreal or scansorial habitat, although at less than a meter in length and under 2 kg, *Dromomeron* is still small enough to forage terrestrially under cover of foliage as well. This suggests that small basal ornithodirans may have been restricted at high latitudes to areas of dense vegetation. *Hesperosuchus* is also restricted to 100% shade seeking behavior from November through April. At 18 kg, foraging under cover of foliage would have been more difficult, raising the possibility of seasonal dormancy, as seen in brumating extant crocodylians [181].

With burrowing enabled the mammalianomorph can effectively thermoregulate year-round. From November through March time spent in burrow or under shade increases, and in December and January non-shaded foraging time shrinks to as low as two hours a day. With hibernation potentially playing an important role in the origin of mammalian endothermy [182,183] a period of seasonal dormancy cannot be ruled out and should perhaps be expected.

The last burrowing taxon, the rhynchosaur, performs much worse at high latitude. While able to maintain a reduced T_{core} (down to 26 °C from a target of 30 °C) from April to mid-October, the remaining four months require an implausible amount of ME to maintain even the lower T_{core} range, without leaving its burrow. Some form of brumation would be necessary during these months to reduce metabolic energy costs when foraging became impossible.

Coelophysis effectively thermoregulates 24 h a day year-round. The lack of heat stress at high latitudes during the day in summer months raises the intriguing possibility that closely related species might vary drastically in circadian rhythm, something seen in congeneric lizards today [184]. The other non-burrowing dinosaur, *Plateosaurus* also demonstrates the ability to effectively thermoregulate year-round. *Plateosaurus* at high latitude performs significantly better than at low latitude, since heat stress inducing midday temperatures are gone. This matches the Late Triassic distribution of dinosaurs, with small-medium sized theropods like *Coelophysis* found in low and high latitude environments, while large sauropodomorph body fossils are only found at higher latitudes (Figure 14; [14]).

Thermal Ecology of Baseline Monsoon Microclimate at High Latitude

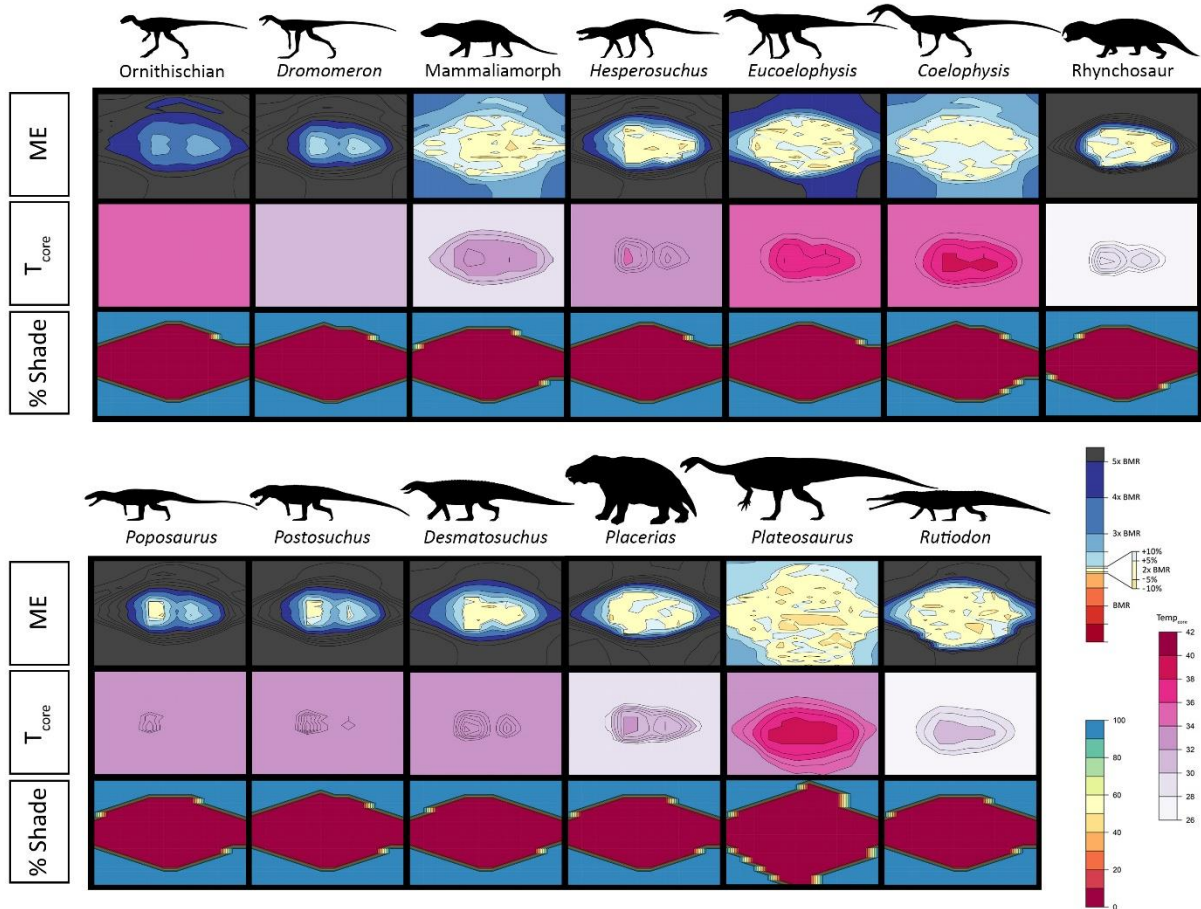


Figure 11. Thermal ecology in a typical Late Triassic seasonal monsoon ecosystem at 55° latitude. Species are arranged from smallest to largest left to right and top to bottom. Full size color keys can be found in Figures 4–7. Abbreviations: ME, metabolic energy; T_{core} , core temperature; %Shade, amount of time per hour an animal must seek out shade to thermoregulate.

Both *Pposaurus* and *Postosuchus* exceed $5\times$ their BMRs to maintain T_{core} at high latitudes year-round, with implausibly high levels of ME being required 24 h a day from October through March. While an ad hoc argument could be made to justify burrowing, this explanation is unnecessary as *Postosuchus* and *Pposaurus* are only known from low latitude environments in the Late Triassic [99,103]. While the relatives of both are known from higher latitudes earlier in the Triassic, it is notable that the more biogeographically diverse relatives of *Pposaurus* seem to either be smaller [88,185], large enough or had elaborated sails that could have raised T_{core} without expending as much ME [186]. An isolated Carnian cervical vertebra referred to the poposaurid *Sillosuchus* suggests a much larger (9–10 m in length, though potentially rare poposaurid living at around 45° paleolatitude, but more anatomical and histological information about *Sillosuchus* will be needed to understand its thermophysiological relationship to its environment.

Desmatosuchus was able to thermoregulate during the day year-round, though from mid-December to mid-January the number of hours of reasonable ME expenditure drop from 6 to 3 h a day. While the year-round foraging ability of *Desmatosuchus* makes it a more plausible inhabitant of high latitudes than *Pposaurus* or *Postosuchus*, it seems likely that some form of brumation would have been necessary during winter months. The extensively armored exterior of aetosaurs would make this a safer proposition, though *Desmatosuchus* itself is only known from low latitudes. Other aetosaurs that lived at higher latitudes such as *Steganolepsis* were smaller and would have been more amenable to

burrowing [97]. Adaptations for scratch-digging [165] reinforce the idea that smaller, high latitude aetosaurs would have used burrowing and seasonal dormancy to survive winters at reasonable ME levels.

Thermal Ecology of Baseline Arid Microclimate at High Latitude

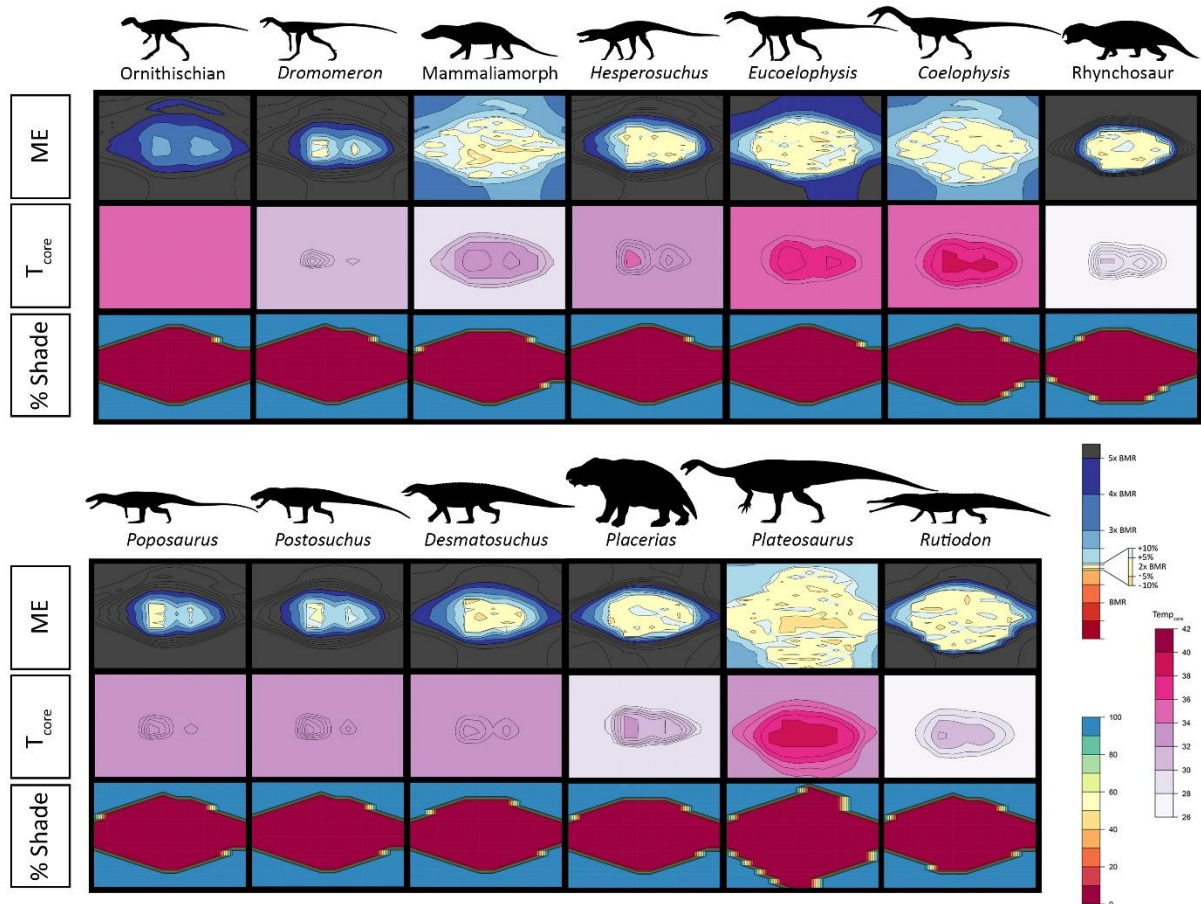


Figure 12. Thermal performance in a Late Triassic arid ecosystem at 55° latitude. Species are arranged from smallest to largest left to right and top to bottom. Full size color keys can be found in Figures 4–7. Abbreviations: ME, metabolic energy; T_{core} , core temperature; %Shade, amount of time per hour an animal must seek out shade to thermoregulate.

Placerias, like *Desmatosuchus* could thermoregulate effectively during midday hours year-round, but experienced cold-stressed ME levels at night, which expand to several hours of morning and evening in December and January. *Placerias* is only known from low latitude deposits, while high latitude Middle and Late Triassic dicynodonts are huge—reaching 4–5 tonnes in size [187]. Smaller and more geographically dispersed dicynodonts have been suggested to utilize burrowing [188,189], but dicynodonts extend back into the Middle Permian [190,191], where they exhibit a wide range of sizes and geographic dispersal, and may have utilized an equally broad array of physiological adaptations [63]. Although beyond the scope of this project, Permian and Early Triassic dicynodonts are rife with opportunity for future thermal ecology modeling.

Rutiodon performs similarly to *Placerias*, though it exhibits more favorable ME rates and non-shade foraging time compared to *Placerias*. *Rutiodon* appears unable to raise T_{core} above 27 °C from October through March. Being too large to burrow, it is unclear whether this would be a viable climate for *Rutiodon*. *Rutiodon* itself is only known from deposits at low paleolatitude, and as the Late Triassic progressed phytosaur remains became progressively

more restricted to low and mid-latitude ecosystems (Figure 14) suggesting that higher latitude cold stress contributed to excluding phytosaurs at high latitudes over time.

Burrowers - Baseline Arid High Latitude

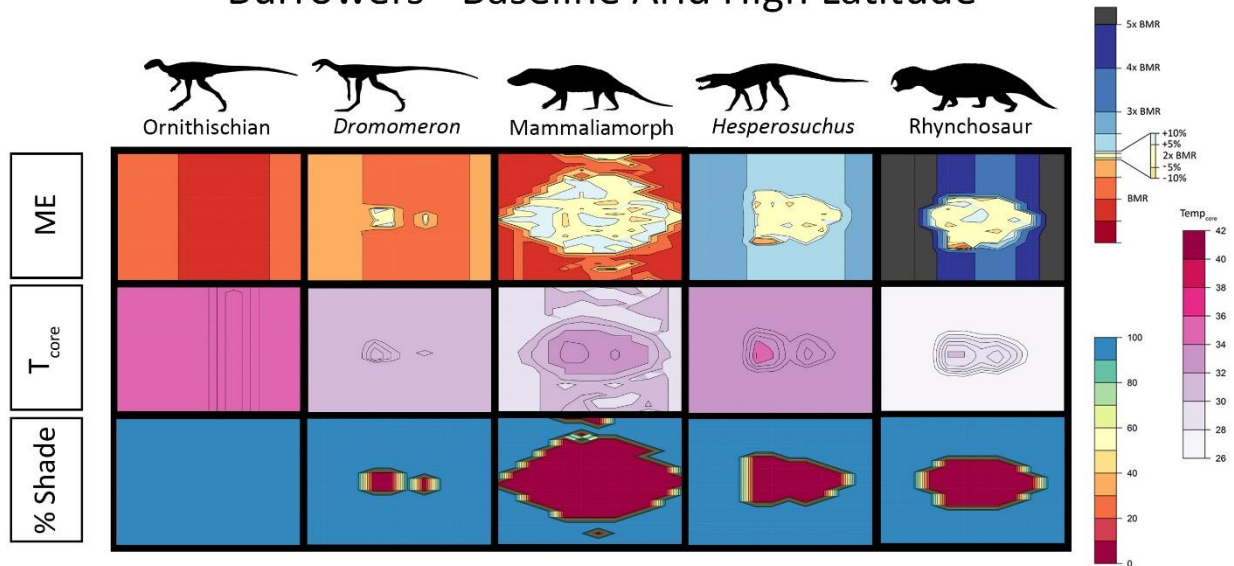


Figure 13. Thermal ecology with burrowing enabled in the baseline arid environment at 55 degrees latitude. Species are arranged from smallest to largest left to right. Red areas in the metabolic energy plots are due to lowered thermoregulation costs while in a burrow, not from heat stress. Full size color keys can be found in Figures 4–7. Abbreviations: ME, metabolic energy; T_{core} , core temperature; %Shade, amount of time per hour an animal must seek out shade to thermoregulate.

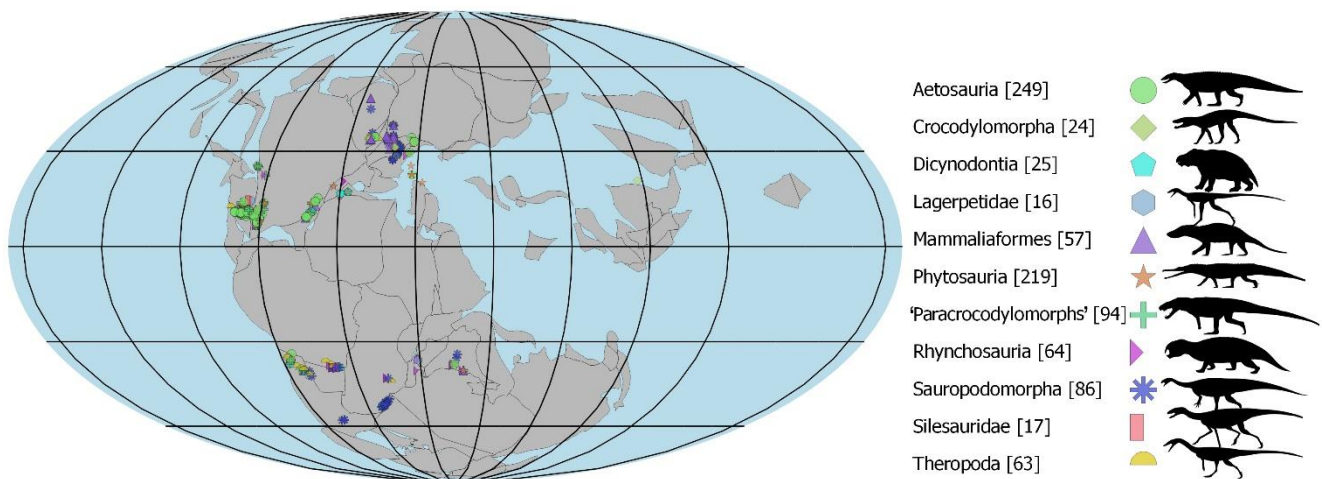


Figure 14. Global distribution of modeled amniote body fossils in the Norian. Occurrence data from paleobiodb.org, continental rotations from glpates.org, silhouettes from phylopic.org (silhouettes not to scale). The label 'Paracrocodylomorphs' denotes a paraphyletic grade including poposauroids and non-crocodylomorph loricatans. Numbers after clade names indicate sample size.

4. Discussion

Mechanistic modeling of thermal ecology in Niche Mapper has successfully predicted thermal tolerance and ranges among extant taxa with a variety of metabolic strategies and masses [4,5,7,35]. Application of Niche Mapper to extinct taxa has recently been vetted for Pleistocene mammals [17,18] and Triassic dinosaurs [14], with the latter combining Niche Mapper’s metabolic chamber function and extensive sensitivity testing to verify its

use in basal theropods and sauropodomorphs. We have applied these tools to examine the thermal ecology of a larger range of 13 Late Triassic taxa.

4.1. Late Triassic Microclimate Results Are Congruous with Previously Inferred Activity Patterns and Fossil Paleobiogeography

Late Triassic microclimate results provide insight into several features of late Triassic ecosystems. While organisms can be assigned activity times (i.e., diurnal, nocturnal, etc.) within Niche Mapper, we left activity time unrestricted during our model runs so thermal constraints rather than behavioral assumptions would drive model taxa activity patterns. Thus, the mammalian morph was found to be nocturnal because its combination of size, burrowing, incipient mammalian endothermy, and mammalian epidermal insulation performed better by being active at night, not due to preexisting hypotheses. Likewise, taxa that were cold-stressed to the point of inactivity during night time hours are considered diurnal. That Niche Mapper's nocturnal mammalian morph results match up with morphological evidence from olfactory and auditory anatomy [59,192] as well as ancestral genetic studies of vision genes [193] provides yet more evidence for the efficacy of mechanistic modeling in extinct vertebrates. The results provide a novel perspective on evolutionary mechanisms in this scenario, suggesting that burrowing and nocturnality evolved in mammalian morphs due to the thermal constraints they encountered, not due to competition with diurnal dinosaurs as is commonly suggested [171,193].

The results contradict the idea of a simple diurnal/nocturnal split between archosaurs and stem-mammals. While some archosaurs like *Poposaurus* and *Desmotosuchus* were restricted to diurnal activity, in low latitudes *Coelophys* was found to be most likely nocturnal, crepuscular, or cathemeral, a result consistent with the activity pattern reconstructed from anatomical data in a close relative [171]. The lack of thermal constraints found on activity time in small burrowing ornithischian dinosaurs suggests the potential for cathemeral activity, while insectivorous silesaurids best functioned within crepuscular activity periods.

These results suggest that thermal ecology is an important driver of paleobiogeographical patterns (Figure 14). It has already been noted that low latitude heat stress on *Plateosaurus* is consistent with large sauropodomorphs being found predominantly at higher latitudes [14], but the restriction to low latitudes of modeled taxa like *Poposaurus* and *Postosuchus* [98,103], as well as the restriction of large phytosaurs like *Rutiodon* to lower latitudes (Figure 14) are all consistent with the fossil record.

4.2. The Importance of Burrowing and Dormancy Are Often Overlooked in Vertebrate Paleoecology

Our results demonstrate the importance of burrowing for small and medium-sized taxa. For small animals this was true regardless of metabolic rate or target T_{core} , while at larger sizes uninsulated or ectothermic taxa were more likely to need the thermal isolation of a burrow to retreat to at night or in colder climates. Even surprisingly large taxa, like the 75 kg *Poposaurus*, which lacks obvious adaptations to burrowing would have been able to more effectively thermoregulate if burrowing had been enabled, especially at high latitudes (e.g., Figures 10–12). This should not be a surprising finding, as using a burrow or other environmental insulation to escape unfavorable thermal conditions is widespread in extant animals [140]. Yet, the physiological importance of utilizing burrows and the impact they have on size evolution and potential barriers to geographic dispersal in Paleozoic and Mesozoic tetrapods are under-discussed, and finding evidence of burrowing in archosaurs has traditionally been treated as an unexpected discovery [153,194].

A similar result is the importance of metabolic dormancy during thermally stressful seasonality. Utilizing some form of metabolic dormancy is widespread among small animals today [195,196] and may have been important to the origin of mammalian sleeping patterns [183]. In the pre-ETE Triassic microclimates, taxa at higher latitude often would have endured lower thermal stress and reduced energy budgets if brumation, torpor, or hibernation were enabled. Incorporating burrows and improved understanding of

metabolic dormancy will likely be key to modeling the paleobiogeographic niches of small vertebrates in high latitudes in Paleozoic and Mesozoic ecosystems.

4.3. Limitations and Future Work

We have focused on adult organisms and their distributions, but have not addressed reproductive success and the requirements for subsurface soil conditions that provide suitable incubation gas exchange, hydric environments, temperatures and their durations for successful hatching, as has been done for the leatherback sea turtle [7], the tuatara [197] and the Western Swamp Tortoise [198]. We have also not yet considered developmental requirements in terms of climates available/necessary for hatchlings and juveniles of the species considered here to flourish in their growth and development to reproductive maturity.

There are also significant opportunities for future research to expand on our thermal ecology modeling of Triassic ecosystems. Several terrestrial Late Triassic tetrapod clades remain unmodeled, particularly among basal archosauromorphs and non-amniote tetrapods. Continued exploration and description of new taxa will add to the geographic and temporal range of modeled clades, providing tests of current assumptions.

Future work may focus on modeling additional latitudes and microclimates, especially the colder and more seasonal eastern and central portions of high-latitude Laurasia. As both species and geographic sampling increases, the predictive power and limitations of thermal ecology modeling should become more clear. Continued publication of additional paleoclimate proxies should lead to the creation of higher fidelity global climate models, providing another avenue for improvement in future research. Finally, modeling competing interpretations of climate disturbance during mass extinction events, like the End Triassic Extinction, offer the potential to test mechanistic explanations for patterns of survivorship during Earth's five mass extinctions [199].

5. Conclusions

Our modeling shows that thermal ecology is sufficient to constrain the latitudinal biogeography of a subset of 13 Late Triassic amniotes. This does not mean that other factors like resource availability had no role, but biogeography was at least partially modulated by temperature-dependent regulatory behaviors and structures. We demonstrate that nocturnal mammaliamorph behavior was likely present and adaptive to modulate thermal stresses in locations where heat stress would have likely excluded the modeled taxa. In addition, thermal stress on small taxa suggest burrowing behavior was necessary to allow for their observed paleogeographic occurrences. Combined, these methods and results show the utility that quantitative thermal ecology modeling has for vertebrate paleobiology and highlights new opportunities for quantitative hypothesis testing in the future.

Supplementary Materials: Available online at <https://figshare.com/s/2ec392df6aed0ecc4d0c>, Figure S1: All Niche Mapper plots (without burrowing), Species are arranged from smallest to largest left to right and top to bottom. Abbreviations: ME, metabolic energy; T_{core} , core temperature; %Shade, amount of time per hour an animal must seek out shade to thermoregulate. Figure S2: All burrowing Niche Mapper plots (burrowing enabled). Species are arranged from smallest to largest left to right. Red areas in the metabolic energy plots are due to lowered thermoregulation costs while in a burrow, not from heat stress. Abbreviations: ME, metabolic energy; T_{core} , core temperature; %Shade, amount of time per hour an animal must seek out shade to thermoregulate. Table S1: Complete microclimate input file. Table S2: Complete biophysical input file. Table S3: Raw output files from Niche Mapper, prior to collating into plots in S1, S2 and Figures 8–13.

Author Contributions: Conceptualization, S.A.H., D.M.L. and W.P.P.; methodology, S.A.H., D.M.L., B.J.L., P.D.M. and W.P.P.; software, W.P.P., P.D.M., B.J.L., D.M.L. and S.A.H.; validation, S.A.H., D.M.L., B.J.L., P.D.M. and W.P.P.; formal analysis, S.A.H. and D.M.L.; investigation, S.A.H., D.M.L. and W.P.P.; resources; data curation, S.A.H.; writing—original draft preparation, S.A.H.; writing—review and editing, S.A.H., D.M.L., B.J.L., P.D.M. and W.P.P.; visualization, S.A.H., D.M.L. and B.J.L. All authors have read and agreed to the published version of the manuscript.

Funding: This research received no external funding.

Data Availability Statement: All data is provided in the Supplementary Materials.

Acknowledgments: S.H. thanks Shanan Peters and his graduate committee for their advice during initial drafts of this material. We give thanks to all authors that provide well-documented dimensions in their morphological descriptions. Finally, we thank the detailed and insightful work of three anonymous reviewers, whose efforts significantly improved the final manuscript.

Conflicts of Interest: The authors declare no conflict of interest.

References

- Barlett, P.N.; Gates, D.M. The Energy Budget of a Lizard on a Tree Trunk. *Ecology* **1967**, *48*, 315–322. [[CrossRef](#)]
- Levy, O.; Dayan, T.; Kronfeld-Schor, N.; Porter, W.P. Biophysical Modeling of the Temporal Niche: From First Principles to the Evolution of Activity Patterns. *Am. Nat.* **2012**, *179*, 794–804. [[CrossRef](#)] [[PubMed](#)]
- Dudley, P.; Bonazza, R.; Porter, W. Consider a Non-Spherical Elephant: Computational Fluid Dynamics Simulations of Heat Transfer Coefficients and Drag Verified Using Wind Tunnel Experiments. *J. Exp. Zool. Part Ecol. Genet. Physiol.* **2013**, *319*, 319–327. [[CrossRef](#)] [[PubMed](#)]
- Kearney, M.; Porter, W. Mechanistic Niche Modelling: Combining Physiological and Spatial Data to Predict Species' Ranges. *Ecol. Lett.* **2009**, *12*, 334–350. [[CrossRef](#)] [[PubMed](#)]
- Mathewson, P.D.; Porter, W.P. Simulating Polar Bear Energetics during a Seasonal Fast Using a Mechanistic Model. *PLoS ONE* **2013**, *8*, e72863. [[CrossRef](#)] [[PubMed](#)]
- Fitzpatrick, M.J.; Mathewson, P.D.; Porter, W.P. Validation of a Mechanistic Model for Non-Invasive Study of Ecological Energetics in an Endangered Wading Bird with Counter-Current Heat Exchange in Its Legs. *PLoS ONE* **2015**, *10*, e0136677. [[CrossRef](#)]
- Dudley, P.; Bonazza, R.; Porter, W. Climate Change Impacts on Nesting and Internesting Leatherback Sea Turtles Using 3D Animated Computational Fluid Dynamics and Finite Volume Heat Transfer. *Ecol. Model.* **2016**, *320*, 231–240. [[CrossRef](#)]
- Porter, W.P.; Gates, D.M. Thermodynamic Equilibria of Animals with Environment. *Ecol. Monogr.* **1969**, *39*, 227–244. [[CrossRef](#)]
- Spotila, J.R.; Lommen, P.W.; Bakken, G.S.; Gates, D.M. A Mathematical Model for Body Temperatures of Large Reptiles: Implications for Dinosaur Ecology. *Am. Nat.* **1973**, *107*, 391–404. [[CrossRef](#)]
- Skoczytas, R. Thermoregulation in Dinosaurs. In *Contributions to Thermal Physiology*; Elsevier: Amsterdam, The Netherlands, 1981; pp. 249–251.
- Dunham, A.; Overall, K.; Porter, W.; Forster, C. Implications of Ecological Energetic and Biophysical and Developmental Constraints for Life-History Variation in Dinosaurs. In *Paleobiology of the Dinosaurs*; Geological Society of America Special: Boulder, CO, USA, 1989; Volume 238, pp. 1–21. ISBN 978-0-8137-2238-2.
- Long, R.A.; Bowyer, R.T.; Porter, W.P.; Mathewson, P.; Monteith, K.L.; Findholt, S.L.; Dick, B.L.; Kie, J.G. Linking Habitat Selection to Fitness-Related Traits in Herbivores: The Role of the Energy Landscape. *Oecologia* **2016**, *181*, 709–720. [[CrossRef](#)]
- Lin, T.-E.; Chen, T.-Y.; Wei, H.-L.; Richard, R.; Huang, S.-P. Low Cold Tolerance of the Invasive Lizard *Eutropis Multifasciata* Constrains Its Potential Elevation Distribution in Taiwan. *J. Therm. Biol.* **2019**, *82*, 115–122. [[CrossRef](#)] [[PubMed](#)]
- Lovelace, D.M.; Hartman, S.A.; Mathewson, P.D.; Linzmeier, B.J.; Porter, W.P. Modeling Dragons: Using Linked Mechanistic Physiological and Microclimate Models to Explore Environmental, Physiological, and Morphological Constraints on the Early Evolution of Dinosaurs. *PLoS ONE* **2020**, *15*, e0223872. [[CrossRef](#)] [[PubMed](#)]
- Hartman, S.; Lovelace, D.; Linzmeier, B.; Porter, W. Using Ecological Modelling to Quantify Thermal Constraints on Two Late Triassic Dinosaurs. *J. Vertebr. Paleontol.* **2015**, *36*, 139.
- Hartman, S.; Lovelace, D.; Linzmeier, B.; Mathewson, P.; Porter, W. Mechanistic Physiological Modelling Predicts Geographic Distribution of Late Triassic Tetrapods. *J. Vertebr. Paleontol.* **2016**, *35*.
- Mathewson, P.D.; Moyer-Horner, L.; Beaver, E.A.; Briscoe, N.J.; Kearney, M.; Yahn, J.M.; Porter, W.P. Mechanistic Variables Can Enhance Predictive Models of Endotherm Distributions: The American Pika under Current, Past, and Future Climates. *Glob. Chang. Biol.* **2017**, *23*, 1048–1064. [[CrossRef](#)]
- Wang, Y.; Porter, W.; Mathewson, P.D.; Miller, P.A.; Graham, R.W.; Williams, J.W. Mechanistic Modeling of Environmental Drivers of Woolly Mammoth Carrying Capacity Declines on St. Paul Island. *Ecology* **2018**, *99*, 2721–2730. [[CrossRef](#)]
- Wang, Y.; Widga, C.; Graham, R.W.; McGuire, J.L.; Porter, W.; Wårlind, D.; Williams, J.W. Caught in a Bottleneck: Habitat Loss for Woolly Mammoths in Central North America and the Ice-Free Corridor during the Last Deglaciation. *Glob. Ecol. Biogeogr.* **2021**, *30*, 527–542. [[CrossRef](#)]
- Porter, W.; Mitchell, J. Method and System for Calculating the Spatial-Temporal Effects of Climate and Other Environmental Conditions on Animals. In *Office Up*, Editor; 11-0E Wisconsin Alumni Research Foundation: Madison, WI, USA, 2006.
- R Core Team. *R: A Language and Environment for Statistical Computing*; R Foundation for Statistical Computing: Vienna, Austria, 2020.
- Urbanek, S. *Png: Read and Write PNG Images*, 2013.
- Warnes, G.R.; Bolker, B.; Bonebakker, L.; Gentleman, R.; Liaw, W.H.A.; Lumley, T. *Package 'Gplots': Various r Programming Tools for Plotting Data*, R Package Version 3.0.1. 2016.

24. Wickham, H. *Ggplot2: Elegant Graphics for Data Analysis*; Springer: Berlin/Heidelberg, Germany, 2016.
25. Neuwirth, E.; Neuwirth, M.E. Package 'RColorBrewer'. *Color. Palettes* **2014**.
26. Lemon, J. Plotrix: A Package in the Red Light District of R. *R-News* **2006**, *6*, 8–12.
27. QGIS Development Team. *QGIS Geographic Information System*, 2019.
28. Laskar, J.; Robutel, P.; Joutel, F.; Gastineau, M.; Correia, A.C.M.; Levrard, B. A Long-Term Numerical Solution for the Insolation Quantities of the Earth. *Astron. Astrophys.* **2004**, *428*, 261–285. [[CrossRef](#)]
29. Crucifix, M. *Palinsol: Insolation for Palaeoclimate Studies*, 2016.
30. Geiger, R.; Aron, R.H.; Todhunter, P. *The Climate near the Ground*; Rowman & Littlefield: Lanham, MD, USA, 2009.
31. McCullough, E.C.; Porter, W.P. Computing Clear Day Solar Radiation Spectra for the Terrestrial Ecological Environment. *Ecology* **1971**, *52*, 1008–1015. [[CrossRef](#)]
32. Porter, W.P.; Mitchell, J.W.; Beckman, W.A.; DeWitt, C.B. Behavioral Implications of Mechanistic Ecology. *Oecologia* **1973**, *13*, 1–54. [[CrossRef](#)] [[PubMed](#)]
33. Kearney, M.R.; Shamakhly, A.; Tingley, R.; Karoly, D.J.; Hoffmann, A.A.; Briggs, P.R.; Porter, W.P. Microclimate Modelling at Macro Scales: A Test of a General Microclimate Model Integrated with Gridded Continental-Scale Soil and Weather Data. *Methods Ecol. Evol.* **2014**, *5*, 273–286. [[CrossRef](#)]
34. Porter, W.P.; Vakharia, N.; Klousie, W.D.; Duffy, D. Po'ouli Landscape Bioinformatics Models Predict Energetics, Behavior, Diets, and Distribution on Maui. *Integr. Comp. Biol.* **2006**, *46*, 1143–1158. [[CrossRef](#)]
35. Long, R.A.; Bowyer, R.T.; Porter, W.P.; Mathewson, P.; Monteith, K.L.; Kie, J.G. Behavior and Nutritional Condition Buffer a Large-Bodied Endotherm against Direct and Indirect Effects of Climate. *Ecol. Monogr.* **2014**, *84*, 513–532. [[CrossRef](#)]
36. Sellwood, B.W.; Valdes, P.J. Mesozoic Climates: General Circulation Models and the Rock Record. *Sediment. Geol.* **2006**, *190*, 269–287. [[CrossRef](#)]
37. Landwehrs, J.P.; Feulner, G.; Hofmann, M.; Petri, S. Climatic Fluctuations Modeled for Carbon and Sulfur Emissions from End-Triassic Volcanism. *Earth Planet. Sci. Lett.* **2020**, *537*, 116174. [[CrossRef](#)]
38. Kutzbach, J. Idealized Pangean Climates: Sensitivity to Orbital Change. In *Pangea: Paleoclimate, Tectonics, and Sedimentation During Accretion, Zenith, and Breakup of a Supercontinent*; Klein, G., Ed.; Geological Society of America: Boulder, CO, USA, 1994; ISBN 978-0-8137-2288-7.
39. Kustatscher, E.; Ash, S.R.; Karasev, E.; Pott, C.; Vajda, V.; Yu, J.; McLoughlin, S. Flora of the Late Triassic. In *The Late Triassic World: Earth in a Time of Transition*; Tanner, L.H., Ed.; Topics in Geobiology; Springer International Publishing: Cham, Switzerland, 2018; pp. 545–622. ISBN 978-3-319-68009-5.
40. Mancuso, A.C.; Horn, B.L.D.; Benavente, C.A.; Schultz, C.L.; Irmis, R.B. The Paleoclimatic Context for South American Triassic Vertebrate Evolution. *J. S. Am. Earth Sci.* **2021**, *110*, 103321. [[CrossRef](#)]
41. Olsen, P.; Sha, J.; Fang, Y.; Chang, C.; Whiteside, J.H.; Kinney, S.; Sues, H.-D.; Kent, D.; Schaller, M.; Vajda, V. Arctic Ice and the Ecological Rise of the Dinosaurs. *Sci. Adv.* **2022**, *8*, eabo6342. [[CrossRef](#)]
42. Parrish, J.T. Climate of the Supercontinent Pangea. *J. Geol.* **1993**, *101*, 215–233. [[CrossRef](#)]
43. Timbuktu Climate, Weather by Month, Average Temperature (Mali)—Weather Spark. Available online: <https://weatherspark.com/y/36520/Average-Weather-in-Timbuktu-Mali-Year-Round> (accessed on 1 April 2022).
44. Tamale Climate, Weather by Month, Average Temperature (Ghana)—Weather Spark. Available online: <https://weatherspark.com/y/42343/Average-Weather-in-Tamale-Ghana-Year-Round> (accessed on 1 April 2022).
45. Berner, R.A.; Beerling, D.J.; Dudley, R.; Robinson, J.M.; Wildman, R.A. Phanerozoic Atmospheric Oxygen. *Annu. Rev. Earth Planet. Sci.* **2003**, *31*, 105–134. [[CrossRef](#)]
46. Cleveland, D.M.; Nordt, L.C.; Atchley, S.C. Paleosols, Trace Fossils, and Precipitation Estimates of the Uppermost Triassic Strata in Northern New Mexico. *Palaeogeogr. Palaeoclimatol. Palaeoecol.* **2008**, *257*, 421–444. [[CrossRef](#)]
47. Berner, R.A.; Kothavala, Z. Geocarb III: A Revised Model of Atmospheric CO₂ over Phanerozoic Time. *Am. J. Sci.* **2001**, *301*, 182–204. [[CrossRef](#)]
48. Peczkis, J. Implications of Body-Mass Estimates for Dinosaurs. *J. Vertebr. Paleontol.* **1995**, *14*, 520–533. [[CrossRef](#)]
49. Paul, G.S. Dinosaur Models: The Good, the Bad, and Using Them to Estimate the Mass of Dinosaurs. In *DinoFest International Proceedings*; Academy of Natural Science: Philadelphia, PA, USA, 1997; pp. 129–154.
50. Seebacher, F. A New Method to Calculate Allometric Length-Mass Relationships of Dinosaurs. *J. Vertebr. Paleontol.* **2001**, *21*, 51–60. [[CrossRef](#)]
51. Farlow, J.O.; Holtz, T.R. The Fossil Record of Predation in Dinosaurs. *Paleontol. Soc. Pap.* **2002**, *8*, 251–266. [[CrossRef](#)]
52. Melstrom, K.M.; Irmis, R.B. Repeated Evolution of Herbivorous Crocodyliforms during the Age of Dinosaurs. *Curr. Biol.* **2019**, *29*, 2389–2395. [[CrossRef](#)]
53. Porter, W.P.; Kearney, M. Size, Shape, and the Thermal Niche of Endotherms. *Proc. Natl. Acad. Sci. USA* **2009**, *106*, 19666–19672. [[CrossRef](#)]
54. Kearney, M.R.; Briscoe, N.J.; Mathewson, P.D.; Porter, W.P. NicheMapR—An R Package for Biophysical Modelling: The Endotherm Model. *Ecography* **2021**, *44*, 1595–1605. [[CrossRef](#)]
55. Bennett, A.F. Activity Metabolism of the Lower Vertebrates. *Annu. Rev. Physiol.* **1978**, *40*, 447–469. [[CrossRef](#)]
56. McKechnie, A.E.; Wolf, B.O. The Allometry of Avian Basal Metabolic Rate: Good Predictions Need Good Data. *Physiol. Biochem. Zool.* **2004**, *77*, 502–521. [[CrossRef](#)] [[PubMed](#)]

57. Sulej, T.; Niedźwiedzki, G. An Elephant-Sized Late Triassic Synapsid with Erect Limbs. *Science* **2019**, *363*, 78–80. [[CrossRef](#)] [[PubMed](#)]
58. Liu, Y.; Chi, H.; Li, L.; Rossiter, S.J.; Zhang, S. Molecular Data Support an Early Shift to an Intermediate-Light Niche in the Evolution of Mammals. *Mol. Biol. Evol.* **2018**, *35*, 1130–1134. [[CrossRef](#)] [[PubMed](#)]
59. Luo, Z.-X.; Meng, Q.-J.; Ji, Q.; Liu, D.; Zhang, Y.-G.; Neander, A.I. Evolutionary Development in Basal Mammaliaforms as Revealed by a Docodontan. *Science* **2015**, *347*, 760–764. [[CrossRef](#)] [[PubMed](#)]
60. Ji, Q.; Luo, Z.-X.; Yuan, C.-X.; Tabrum, A.R. A Swimming Mammaliaform from the Middle Jurassic and Ecomorphological Diversification of Early Mammals. *Science* **2006**, *311*, 1123–1127. [[CrossRef](#)]
61. Fiorillo, A.R.; Padian, K.; Musikasinthorn, C. Taphonomy and Depositional Setting of the Placerias Quarry (Chinle Formation: Late Triassic, Arizona). *Palaios* **2000**, *15*, 373–386. [[CrossRef](#)]
62. Pond, C.M. An Evolutionary and Functional View of Mammalian Adipose Tissue. *Proc. Nutr. Soc.* **1992**, *51*, 367–377. [[CrossRef](#)]
63. Botha-Brink, J.; Angielczyk, K.D. Do Extraordinarily High Growth Rates in Permo-Triassic Dicotylodonts (Therapsida, Anomodontia) Explain Their Success before and after the End-Permian Extinction? *Zool. J. Linn. Soc.* **2010**, *160*, 341–365. [[CrossRef](#)]
64. Rey, K.; Amiot, R.; Fourel, F.; Abdala, F.; Fluteau, F.; Jalil, N.-E.; Liu, J.; Rubidge, B.S.; Smith, R.M.; Steyer, J.S.; et al. Oxygen Isotopes Suggest Elevated Thermometabolism within Multiple Permo-Triassic Therapsid Clades. *eLife* **2017**, *6*, e28589. [[CrossRef](#)]
65. Bajdek, P.; Owocki, K.; Niedźwiedzki, G. Putative Dicotylodont Coprolites from the Upper Triassic of Poland. *Palaeogeogr. Palaeoclimatol. Palaeoecol.* **2014**, *411*, 1–17. [[CrossRef](#)]
66. McNab, B.K. An Analysis of the Factors That Influence the Level and Scaling of Mammalian BMR. *Comp. Biochem. Physiol. A. Mol. Integr. Physiol.* **2008**, *151*, 5–28. [[CrossRef](#)] [[PubMed](#)]
67. Bajdek, P.; Qvarnström, M.; Owocki, K.; Sulej, T.; Sennikov, A.G.; Golubev, V.K.; Niedźwiedzki, G. Microbiota and Food Residues Including Possible Evidence of Pre-Mammalian Hair in Upper Permian Coprolites from Russia. *Lethaia* **2016**, *49*, 455–477. [[CrossRef](#)]
68. Rowe, T. Definition, Diagnosis, and Origin of Mammalia. *J. Vertebr. Paleontol.* **1988**, *8*, 241–264. [[CrossRef](#)]
69. Luo, Z.-X. Transformation and Diversification in Early Mammal Evolution. *Nature* **2007**, *450*, 1011–1019. [[CrossRef](#)]
70. Datta, P.M. Earliest Mammal with Transversely Expanded Upper Molar from the Late Triassic (Carnian) Tiki Formation, South Rewa Gondwana Basin, India. *J. Vertebr. Paleontol.* **2005**, *25*, 200–207. [[CrossRef](#)]
71. Kielan-Jaworowska, Z.; Cifelli, R.L.; Luo, Z.-X. *Mammals from the Age of Dinosaurs: Origins, Evolution, and Structure*; Columbia University Press: New York, NY, USA, 2005; ISBN 978-0-231-11918-4.
72. Hammer, W.R.; Smith, N.D. A Tritylodont Postcanine from the Hanson Formation of Antarctica. *J. Vertebr. Paleontol.* **2008**, *28*, 269–273. [[CrossRef](#)]
73. Kemp, T.S. *The Origin and Evolution of Mammals*; Oxford University Press on Demand: Oxford, UK, 2005.
74. Matsuoka, H.; Kusuhashi, N.; Corfe, I.J. A New Early Cretaceous Tritylodontid (Synapsida, Cynodontia, Mammaliaforma) from the Kuwajima Formation (Tetori Group) of Central Japan. *J. Vertebr. Paleontol.* **2016**, *36*, e1112289. [[CrossRef](#)]
75. Araújo, R.; David, R.; Benoit, J.; Lungmus, J.K.; Stoessel, A.; Barrett, P.M.; Maisano, J.A.; Ekdale, E.; Orliac, M.; Luo, Z.-X.; et al. Inner Ear Biomechanics Reveals a Late Triassic Origin for Mammalian Endothermy. *Nature* **2022**, *607*, 726–731. [[CrossRef](#)]
76. Newham, E.; Gill, P.G.; Brewer, P.; Benton, M.J.; Fernandez, V.; Gostling, N.J.; Habberthür, D.; Jernvall, J.; Kankaanpää, T.; Kallonen, A.; et al. Reptile-like Physiology in Early Jurassic Stem-Mammals. *Nat. Commun.* **2020**, *11*, 5121. [[CrossRef](#)]
77. Sues, H.-D. *Skull and Dentition of Two Tritylodontid Synapsids from the Lower Jurassic of Western North America*; Harvard University: Cambridge, MA, USA, 1986.
78. Hu, Y.; Meng, J.; Clark, J.M. A New Tritylodontid from the Upper Jurassic of Xinjiang, China. *Acta Palaeontol. Pol.* **2009**, *54*, 385–391. [[CrossRef](#)]
79. Nowak, R.M.; Walker, E.P. *Walker's Mammals of the World*; JHU Press: Baltimore, MD, USA, 1999; Volume 1.
80. Ezcurra, M.D. The Phylogenetic Relationships of Basal Archosauromorphs, with an Emphasis on the Systematics of Proterosuchian Archosauriforms. *PeerJ* **2016**, *4*, e1778. [[CrossRef](#)] [[PubMed](#)]
81. Mukherjee, D.; Ray, S. A New *Hyperodapedon* (Archosauromorpha, Rhynchosauria) from the Upper Triassic of India: Implications for Rhynchosaur Phylogeny. *Palaeontology* **2014**, *57*, 1241–1276. [[CrossRef](#)]
82. de Ricqlès, A.; Padian, K.; Knoll, F.; Horner, J.R. On the Origin of High Growth Rates in Archosaurs and Their Ancient Relatives: Complementary Histological Studies on Triassic Archosauriforms and the Problem of a “Phylogenetic Signal” in Bone Histology. In *Annales de Paléontologie*; Elsevier: Amsterdam, The Netherlands, 2008; Volume 94, pp. 57–76.
83. Botha-Brink, J.; Smith, R.M. Osteohistology of the Triassic Archosauromorphs *Prolacerta*, *Proterosuchus*, *Euparkeria*, and *Erythrosuchus* from the Karoo Basin of South Africa. *J. Vertebr. Paleontol.* **2011**, *31*, 1238–1254. [[CrossRef](#)]
84. Veiga, F.H.; Soares, M.B.; Sayão, J.M. Osteohistology of Hyperodapedontine Rhynchosaurs from the Upper Triassic of Southern Brazil. *Acta Palaeontol. Pol.* **2014**, *60*, 829–836.
85. Traeholt, C. Notes on the Burrows of the Water Monitor Lizard, *Varanus salvator*. *Malay. Nat. J.* **1995**, *49*, 103–112.
86. Lutz, R.L.; Lutz, J.M. *Komodo, the Living Dragon*; Dimi Press: Portland, OR, USA, 1997; ISBN 978-0-931625-27-5.
87. Stevenson, R.D. The Relative Importance of Behavioral and Physiological Adjustments Controlling Body Temperature in Terrestrial Ectotherms. *Am. Nat.* **1985**, *126*, 362–386. [[CrossRef](#)]
88. Nesbitt, S.J.; Desojo, J.B.; Irmis, R.B. Anatomy, Phylogeny and Palaeobiology of Early Archosaurs and Their Kin. *Geol. Soc. Lond. Spec. Publ.* **2013**, *379*, 1–7. [[CrossRef](#)]

89. Brusatte, S.L.; Benton, M.J.; Desojo, J.B.; Langer, M.C. The Higher-Level Phylogeny of Archosauria (Tetrapoda: Diapsida). *J. Syst. Palaeontol.* **2010**, *8*, 3–47. [[CrossRef](#)]
90. Padian, K.; Li, C.; Pchelnykova, J. The Trackmaker of *Apatopus* (Late Triassic, North America): Implications for the Evolution of Archosaur Stance and Gait. *Palaeontology* **2010**, *53*, 175–189. [[CrossRef](#)]
91. de Ricqlès, A.J.; Padian, K.; Horner, J.R. On the Bone Histology of Some Triassic Pseudosuchian Archosaurs and Related Taxa. In *Annales de Paléontologie*; Elsevier: Amsterdam, The Netherlands, 2003; Volume 89, pp. 67–101.
92. Scheyer, T.M.; Desojo, J.B.; Cerda, I.A. Bone Histology of Phytosaur, Aetosaur, and Other Archosauriform Osteoderms (Eureptilia, Archosauromorpha). *Anat. Rec.* **2014**, *297*, 240–260. [[CrossRef](#)]
93. Huene, F.R. *A New Phytosaur from the Palisades near New York*; Bulletin of the AMNH, American Museum of Natural History: New York, NY, USA, 1913; Volume 32, p. 15.
94. Hurlburt, G.R.; Heckert, A.B.; Farlow, J.O. Body Mass Estimates of Phytosaurs (Archosauria: Parasuchidae) from the Petrified Forest Formation (Chinle Group: Revueltian) Based on Skull and Limb Bone Measurements. *New Mex. Mus. Nat. Hist. Sci. Bull.* **2003**, *24*, 105–113.
95. Desojo, J.; Ezcurra, M.; Kischlat, E.E. A New Aetosaur Genus (Archosauria: Pseudosuchia) from the Early Late Triassic of Southern Brazil. *Zootaxa* **2012**, *3166*, 1–33. [[CrossRef](#)]
96. Small, B.J. The Triassic Thecodontian Reptile *Desmatosuchus*: Osteology and Relationships. Ph.D. Thesis, Texas Tech University, Lubbock, TX, USA, 1985.
97. Walker, A.D. Triassic Reptiles from the Elgin Area: *Stagonolepis*, *Dasygnathus* and Their Allies. *Philos. Trans. R. Soc. Lond. B. Biol. Sci.* **1961**, *244*, 103–204.
98. Gauthier, J.A.; Nesbitt, S.J.; Schachner, E.R.; Bever, G.S.; Joyce, W.G. The Bipedal Stem Crocodylian *Poposaurus Gracilis*: Inferring Function in Fossils and Innovation in Archosaur Locomotion. *Bull. Peabody Mus. Nat. Hist.* **2011**, *52*, 107–126. [[CrossRef](#)]
99. Schachner, E.R.; Irmis, R.B.; Huttenlocker, A.K.; Sanders, K.; Cieri, R.L.; Nesbitt, S.J. Osteology of the Late Triassic Bipedal Archosaur *Poposaurus Gracilis* (Archosauria: Pseudosuchia) from Western North America. *Anat. Rec.* **2020**, *303*, 874–917. [[CrossRef](#)] [[PubMed](#)]
100. Clarke, A.; Pörtner, H.-O. Temperature, Metabolic Power and the Evolution of Endothermy. *Biol. Rev.* **2010**, *85*, 703–727. [[CrossRef](#)]
101. Nesbitt, S. The Anatomy of *Effigia Okeeffeae* (Archosauria, Suchia), Theropod-like Convergence, and the Distribution of Related Taxa. *Bull. Am. Mus. Nat. Hist.* **2007**, *2007*, 1–84. [[CrossRef](#)]
102. Chatterjee, S. *Postosuchus*, a New Thecodontian Reptile from the Triassic of Texas and the Origin of Tyrannosaurs. *Philos. Trans. R. Soc. Lond. B Biol. Sci.* **1985**, *309*, 395–460.
103. Weinbaum, J.C. Postcranial Skeleton of *Postosuchus Kirkpatricki* (Archosauria: Paracrocodylomorpha), from the Upper Triassic of the United States. *Geol. Soc. Lond. Spec. Publ.* **2013**, *379*, 525–553. [[CrossRef](#)]
104. Legendre, L.J.; Segalen, L.; Cubo, J. Evidence for High Bone Growth Rate in *Euparkeria* Obtained Using a New Paleohistological Inference Model for the Humerus. *J. Vertebr. Paleontol.* **2013**, *33*, 1343–1350. [[CrossRef](#)]
105. Klein, N.; Foth, C.; Schoch, R.R. Preliminary Observations on the Bone Histology of the Middle Triassic Pseudosuchian Archosaur *Batrachotomus Kupferzellensis* Reveal Fast Growth with Lamellar Fibrolamellar Bone Tissue. *J. Vertebr. Paleontol.* **2017**, *37*, e1333121. [[CrossRef](#)]
106. Clark, J.M.; Sues, H.-D.; Berman, D.S. A New Specimen of *Hesperosuchus Agilis* from the Upper Triassic of New Mexico and the Interrelationships of Basal Crocodylomorph Archosaurs. *J. Vertebr. Paleontol.* **2001**, *20*, 683–704. [[CrossRef](#)]
107. Lecuona, A.; Desojo, J.B. Hind Limb Osteology of *Gracilisuchus Stipaniceorum* (Archosauria: Pseudosuchia). *Earth Environ. Sci. Trans. R. Soc. Edinb.* **2012**, *102*, 105–128. [[CrossRef](#)]
108. Colbert, E.H. *A Pseudosuchian Reptile from Arizona*; American Museum of Natural History: New York, NY, USA, 1952; Volume 99.
109. Myhrvold, N.P. Dinosaur Metabolism and the Allometry of Maximum Growth Rate. *PLoS ONE* **2016**, *11*, e0163205. [[CrossRef](#)] [[PubMed](#)]
110. Leigh, S.R. Evolution of Human Growth. *Evol. Anthropol. Issues News Rev. Issues News Rev.* **2001**, *10*, 223–236. [[CrossRef](#)]
111. Seymour, R.S.; Bennett-Stamper, C.L.; Johnston, S.D.; Carrier, D.R.; Grigg, G.C. Evidence for Endothermic Ancestors of Crocodiles at the Stem of Archosaur Evolution. *Physiol. Biochem. Zool.* **2004**, *77*, 1051–1067. [[CrossRef](#)]
112. Legendre, L. Did Crocodiles Become Secondarily Ectothermic? A Paleohistological Approach. Ph.D. Thesis, Université Pierre et Marie Curie-Paris VI, Paris, France, 2014.
113. Molnar, J.L.; Pierce, S.E.; Bhullar, B.-A.S.; Turner, A.H.; Hutchinson, J.R. Morphological and Functional Changes in the Vertebral Column with Increasing Aquatic Adaptation in Crocodylomorphs. *R. Soc. Open Sci.* **2015**, *2*, 150439. [[CrossRef](#)]
114. Gauthier, J. Saurischian Monophyly and the Origin of Birds. *Mem. Calif. Acad. Sci.* **1986**, *8*, 1–55.
115. Brusatte, S.L.; Niedźwiedzki, G.; Butler, R.J. Footprints Pull Origin and Diversification of Dinosaur Stem Lineage Deep into Early Triassic. *Proc. R. Soc. B Biol. Sci.* **2011**, *278*, 1107–1113. [[CrossRef](#)]
116. Ezcurra, M.D.; Nesbitt, S.J.; Bronzati, M.; Dalla Vecchia, F.M.; Agnolin, F.L.; Benson, R.B.J.; Brissón Egli, F.; Cabreira, S.F.; Evers, S.W.; Gentil, A.R.; et al. Enigmatic Dinosaur Precursors Bridge the Gap to the Origin of Pterosauria. *Nature* **2020**, *588*, 445–449. [[CrossRef](#)]
117. Sereno, P.C.; Arcucci, A.B. Dinosaurian Precursors from the Middle Triassic of Argentina: *Lagerpeton Chanarensis*. *J. Vertebr. Paleontol.* **1994**, *13*, 385–399. [[CrossRef](#)]

118. Martínez, R.N.; Apaldetti, C.; Correa, G.A.; Abelín, D. A Norian Lagerpetid Dinosauriform from the Quebrada Del Barro Formation, Northwestern Argentina. *Ameghiniana* **2016**, *53*, 1–13. [[CrossRef](#)]
119. Mallison, H. The Digital *Plateosaurus* I: Body Mass, Mass Distribution, and Posture Assessed Using CAD and CAE on a Digitally Mounted Complete Skeleton. *Palaeontol. Electron.* **2010**, *13*, 8A.
120. Pontzer, H.; Allen, V.; Hutchinson, J.R. Biomechanics of Running Indicates Endothermy in Bipedal Dinosaurs. *PLoS ONE* **2009**, *4*, e7783. [[CrossRef](#)]
121. Eagle, R.A.; Tütken, T.; Martin, T.S.; Tripathi, A.K.; Fricke, H.C.; Connely, M.; Cifelli, R.L.; Eiler, J.M. Dinosaur Body Temperatures Determined from Isotopic (¹³C-¹⁸O) Ordering in Fossil Biominerals. *Science* **2011**, *333*, 443–445. [[CrossRef](#)] [[PubMed](#)]
122. Werner, J.; Griebeler, E.M. Allometries of Maximum Growth Rate versus Body Mass at Maximum Growth Indicate That Non-Avian Dinosaurs Had Growth Rates Typical of Fast Growing Ectothermic Sauropsids. *PLoS ONE* **2014**, *9*, e88834. [[CrossRef](#)] [[PubMed](#)]
123. Irmis, R.; Nesbitt, S.; Padian, K.; Smith, N.; Turner, A. A Late Triassic Dinosauriform Assemblage from New Mexico and the Rise of Dinosaurs. *Science* **2007**, *317*, 358–361. [[CrossRef](#)]
124. Griffin, S.T.; Bano, L.S.; Turner, A.H.; Smith, N.D.; Irmis, R.B.; Nesbitt, S.J. Integrating Gross Morphology and Bone Histology to Assess Skeletal Maturity in Early Dinosauriforms: New Insights from *Dromomeron* (Archosauria: Dinosauriforma). *PeerJ* **2019**, *7*, e6331. [[CrossRef](#)]
125. Cabreira, S.F.; Kellner, A.W.A.; Dias-da-Silva, S.; da Silva, L.R.; Bronzati, M.; de Almeida Marsola, J.C.; Müller, R.T.; de Souza Bittencourt, J.; Batista, B.J.; Raugust, T. A Unique Late Triassic Dinosauriform Assemblage Reveals Dinosaur Ancestral Anatomy and Diet. *Curr. Biol.* **2016**, *26*, 3090–3095. [[CrossRef](#)]
126. Sharov, A.G. New Flying Reptiles from the Mesozoic of Kazakhstan and Kyrgyzstan. *Tr. Paleontol. Instituta SSSR* **1971**, *130*, 104–113.
127. Witton, M.P. Pterosaurs. In *Pterosaurs*; Princeton University Press: Princeton, NJ, USA, 2013.
128. Kellner, A.W.A.; Wang, X.; Tischlinger, H.; de Almeida Campos, D.; Hone, D.W.E.; Meng, X. The Soft Tissue of Jeholopterus (Pterosauria, Anurognathidae, Batrachognathinae) and the Structure of the Pterosaur Wing Membrane. *Proc. R. Soc. B Biol. Sci.* **2010**, *277*, 321–329. [[CrossRef](#)] [[PubMed](#)]
129. Xu, X.; Zheng, X.; You, H. A New Feather Type in a Nonavian Theropod and the Early Evolution of Feathers. *Proc. Natl. Acad. Sci. USA* **2009**, *106*, 832–834. [[CrossRef](#)] [[PubMed](#)]
130. McKellar, R.C.; Chatterton, B.D.E.; Wolfe, A.P.; Currie, P.J. A Diverse Assemblage of Late Cretaceous Dinosaur and Bird Feathers from Canadian Amber. *Science* **2011**, *333*, 1619–1622. [[CrossRef](#)] [[PubMed](#)]
131. Xing, L.; McKellar, R.C.; Xu, X.; Li, G.; Bai, M.; Persons IV, W.S.; Miyashita, T.; Benton, M.J.; Zhang, J.; Wolfe, A.P. A Feathered Dinosaur Tail with Primitive Plumage Trapped in Mid-Cretaceous Amber. *Curr. Biol.* **2016**, *26*, 3352–3360. [[CrossRef](#)]
132. Zheng, X.-T.; You, H.-L.; Xu, X.; Dong, Z.-M. An Early Cretaceous Heterodontosaurid Dinosaur with Filamentous Integumentary Structures. *Nature* **2009**, *458*, 333–336. [[CrossRef](#)]
133. Godefroit, P.; Sinitza, S.M.; Dhouiailly, D.; Bolotsky, Y.L.; Sizov, A.V.; McNamara, M.E.; Benton, M.J.; Spagna, P. A Jurassic Ornithischian Dinosaur from Siberia with Both Feathers and Scales. *Science* **2014**, *345*, 451–455. [[CrossRef](#)]
134. Kundrát, M. When Did Theropods Become Feathered?—Evidence for Pre-Archaeopteryx Feathery Appendages. *J. Exp. Zool. B Mol. Dev. Evol.* **2004**, *302*, 355–364. [[CrossRef](#)]
135. Yang, Z.; Jiang, B.; McNamara, M.E.; Kearns, S.L.; Pittman, M.; Kaye, T.G.; Orr, P.J.; Xu, X.; Benton, M.J. Pterosaur Integumentary Structures with Complex Feather-like Branching. *Nat. Ecol. Evol.* **2019**, *3*, 24–30. [[CrossRef](#)]
136. Campione, N.E.; Barrett, P.M.; Evans, D.C. On the Ancestry of Feathers in Mesozoic Dinosaurs. In *The Evolution of Feathers*; Springer: Berlin/Heidelberg, Germany, 2020; pp. 213–243.
137. Heath, T.A.; Hedtke, S.M.; Hillis, D.M. Taxon Sampling and the Accuracy of Phylogenetic Analyses. *J. Syst. Evol.* **2008**, *46*, 239.
138. Müller, R.T.; Dias-da-Silva, S. Taxon Sample and Character Coding Deeply Impact Unstable Branches in Phylogenetic Trees of Dinosaurs. *Hist. Biol.* **2019**, *31*, 1089–1092. [[CrossRef](#)]
139. Thorington, R.W., Jr.; Hoffmann, R.S. Family Sciuridae. In *Mammal Species of the World*; Johns Hopkins University Press: Baltimore, MD, USA, 2005; Volume 2, pp. 753–819.
140. Martin, A.J. *The Evolution Underground: Burrows, Bunkers, and the Marvelous Subterranean World Beneath Our Feet*; Reprint ed.; Pegasus Books: Berkeley, CA, USA, 2017.
141. Kammerer, C.F.; Nesbitt, S.J.; Shubin, N.H. The First Silesaurid Dinosauriform from the Late Triassic of Morocco. *Acta Palaeontol. Pol.* **2011**, *57*, 277–284. [[CrossRef](#)]
142. Qvarnström, M.; Wernström, J.V.; Piechowski, R.; Talanda, M.; Ahlberg, P.E.; Niedźwiedzki, G. Beetle-Bearing Coprolites Possibly Reveal the Diet of a Late Triassic Dinosauriform. *R. Soc. Open Sci.* **2019**, *6*, 181042. [[CrossRef](#)]
143. Ezcurra, M.D. A Review of the Systematic Position of the Dinosauriform Archosaur *Eucoelophysis Baldwinii* Sullivan & Lucas, 1999 from the Upper Triassic of New Mexico, USA. *Geodiversitas* **2006**, *28*, 649–684.
144. Irmis, R.B.; Parker, W.G.; Nesbitt, S.J.; Liu, J. Early Ornithischian Dinosaurs: The Triassic Record. *Hist. Biol.* **2007**, *19*, 3–22. [[CrossRef](#)]
145. Agnolín, F.L.; Rozadilla, S. Phylogenetic Reassessment of *Pisanosaurus Mertii* Casamiquela, 1967, a Basal Dinosauriform from the Late Triassic of Argentina. *J. Syst. Palaeontol.* **2018**, *16*, 853–879. [[CrossRef](#)]

146. BUTLER, R.J. The Anatomy of the Basal Ornithischian Dinosaur *Eocursor Parvus* from the Lower Elliot Formation (Late Triassic) of South Africa. *Zool. J. Linn. Soc.* **2010**, *160*, 648–684. [[CrossRef](#)]
147. McPhee, B.; Bordy, E.; Sciscio, L.; Choiniere, J. The Sauropodomorph Biostratigraphy of the Elliot Formation of Southern Africa: Tracking the Evolution Of Sauropodomorpha across the Triassic-Jurassic Boundary. *Acta Palaeontol. Pol.* **2017**, *3*, 441–465. [[CrossRef](#)]
148. Seymour, R.S.; Lillywhite, H.B. Hearts, Neck Posture and Metabolic Intensity of Sauropod Dinosaurs. *Proc. R. Soc. Lond. B Biol. Sci.* **2000**, *267*, 1883–1887. [[CrossRef](#)]
149. Wedel, M.J. Evidence for Bird-like Air Sacs in Saurischian Dinosaurs. *J. Exp. Zool. Part Ecol. Genet. Physiol.* **2009**, *311*, 611–628. [[CrossRef](#)]
150. Seymour, R. Were Dinosaurs Warm-Blooded? *Australas. Sci.* **2013**, *34*, 16–19.
151. McNab, B.K. Ecological Factors Affect the Level and Scaling of Avian BMR. *Comp. Biochem. Physiol. A. Mol. Integr. Physiol.* **2009**, *152*, 22–45. [[CrossRef](#)] [[PubMed](#)]
152. Maloney, S.K. Thermoregulation in Ratites: A Review. *Aust. J. Exp. Agric.* **2008**, *48*, 1293–1301. [[CrossRef](#)]
153. Varricchio, D.J.; Martin, A.J.; Katsura, Y. First Trace and Body Fossil Evidence of a Burrowing, Denning Dinosaur. *Proc. R. Soc. B Biol. Sci.* **2007**, *274*, 1361–1368. [[CrossRef](#)] [[PubMed](#)]
154. Martinez, R.N.; Alcober, O.A. A Basal Sauropodomorph (Dinosauria: Saurischia) from the Ischigualasto Formation (Triassic, Carnian) and the Early Evolution of Sauropodomorpha. *PLoS ONE* **2009**, *4*, e4397. [[CrossRef](#)] [[PubMed](#)]
155. Otero, A.; Cuff, A.R.; Allen, V.; Sumner-Rooney, L.; Pol, D.; Hutchinson, J.R. Ontogenetic Changes in the Body Plan of the Sauropodomorph Dinosaur *Mussaurus Patagonicus* Reveal Shifts of Locomotor Stance during Growth. *Sci. Rep.* **2019**, *9*, 7614. [[CrossRef](#)] [[PubMed](#)]
156. Hendrickx, C.; Hartman, S.A.; Mateus, O. An Overview Of Non-Avian Theropod Discoveries And Classification. *PalArchs J. Vertebr. Palaeontol.* **2015**, *12*, 1–73.
157. Prochnow, S.J.; Nordt, L.C.; Atchley, S.C.; Hudec, M.R. Multi-Proxy Paleosol Evidence for Middle and Late Triassic Climate Trends in Eastern Utah. *Palaeogeogr. Palaeoclimatol. Palaeoecol.* **2006**, *232*, 53–72. [[CrossRef](#)]
158. Peterson, M.E.; Daniel, R.M.; Danson, M.J.; Eisenthal, R. The Dependence of Enzyme Activity on Temperature: Determination and Validation of Parameters. *Biochem. J.* **2007**, *402*, 331–337. [[CrossRef](#)]
159. Angilletta, M.J.; Cooper, B.S.; Schuler, M.S.; Boyles, J.G. The Evolution of Thermal Physiology in Endotherms. *Front. Biosci. E* **2010**, *2*, 861–881.
160. Koteja, P. On the Relation between Basal and Field Metabolic Rates in Birds and Mammals. *Funct. Ecol.* **1991**, *5*, 56–64. [[CrossRef](#)]
161. Ricklefs, R.E.; Konarzewski, M.; Daan, S. The Relationship between Basal Metabolic Rate and Daily Energy Expenditure in Birds and Mammals. *Am. Nat.* **1996**, *147*, 1047–1071. [[CrossRef](#)]
162. Mole, M.A.; Rodrigues D’Araujo, S.; van Aarde, R.J.; Mitchell, D.; Fuller, A. Coping with Heat: Behavioural and Physiological Responses of Savanna Elephants in Their Natural Habitat. *Conserv. Physiol.* **2016**, *4*, cow044. [[CrossRef](#)] [[PubMed](#)]
163. Dubiel, R.; Parrish, J.; Parrish, J.; Good, S. The Pangaean Megamonsoon-Evidence from the Upper Triassic Chinle Formation, Colorado Plateau. *Palaios* **1991**, *6*, 347–370. [[CrossRef](#)]
164. Whiteside, J.H.; Grogan, D.S.; Olsen, P.E.; Kent, D.V. Climatically Driven Biogeographic Provinces of Late Triassic Tropical Pangea. *Proc. Natl. Acad. Sci. USA* **2011**, *108*, 8972–8977. [[CrossRef](#)] [[PubMed](#)]
165. Owen-Smith, N. Assessing the Foraging Efficiency of a Large Herbivore, the Kudu. *South Afr. J. Wildl. Res.-24-Mon. Delayed Open Access* **1979**, *9*, 102–110. [[CrossRef](#)]
166. Plumb, G.E.; Dodd, J.L. Foraging Ecology of Bison and Cattle on a Mixed Prairie: Implications for Natural Area Management. *Ecol. Appl.* **1993**, *3*, 631–643. [[CrossRef](#)]
167. Bahr, A.; Kolber, G.; Kaboth-Bahr, S.; Reinhardt, L.; Friedrich, O.; Pross, J. Mega-Monsoon Variability during the Late Triassic: Re-Assessing the Role of Orbital Forcing in the Deposition of Playa Sediments in the Germanic Basin. *Sedimentology* **2020**, *67*, 951–970. [[CrossRef](#)]
168. Noy-Meir, I. Desert Ecosystems: Higher Trophic Levels. *Annu. Rev. Ecol. Syst.* **1974**, *5*, 195–214. [[CrossRef](#)]
169. Preto, N.; Kustatscher, E.; Wignall, P.B. Triassic Climates—State of the Art and Perspectives. *Palaeogeogr. Palaeoclimatol. Palaeoecol.* **2010**, *290*, 1–10. [[CrossRef](#)]
170. Crompton, A.; Taylor, C.R.; Jagger, J.A. Evolution of Homeothermy in Mammals. *Nature* **1978**, *272*, 333–336. [[CrossRef](#)]
171. Schmitz, L.; Motani, R. Nocturnality in Dinosaurs Inferred from Scleral Ring and Orbit Morphology. *Science* **2011**, *332*, 705–708. [[CrossRef](#)] [[PubMed](#)]
172. Wolfe, J.L.; Bradshaw, D.K.; Chabreck, R.H. Alligator Feeding Habits: New Data and a Review. *Gulf Mex. Sci.* **1987**, *9*, 1. [[CrossRef](#)]
173. Ramezani, J.; Fastovsky, D.E.; Bowring, S.A. Revised Chronostratigraphy of the Lower Chinle Formation Strata in Arizona and New Mexico (USA): High-Precision U-Pb Geochronological Constraints on the Late Triassic Evolution of Dinosaurs. *Am. J. Sci.* **2014**, *314*, 981–1008. [[CrossRef](#)]
174. Krilloff, A.; Germain, D.; Canoville, A.; Vincent, P.; Sache, M.; Laurin, M. Evolution of Bone Microanatomy of the Tetrapod Tibia and Its Use in Palaeobiological Inference. *J. Evol. Biol.* **2008**, *21*, 807–826. [[CrossRef](#)] [[PubMed](#)]
175. Ugalde, G.D.; Müller, R.T.; de Araújo-Júnior, H.I.; Dias-da-Silva, S.; Pinheiro, F.L. A Peculiar Bonebed Reinforces Gregarious Behaviour for the Triassic Dicynodont *Dinodontosaurus*. *Hist. Biol.* **2020**, *32*, 764–772. [[CrossRef](#)]

176. Fiorelli, L.E.; Ezcurra, M.D.; Hechenleitner, E.M.; Argañaraz, E.; Taborda, J.R.A.; Trotteyn, M.J.; von Baczko, M.B.; Desojo, J.B. The Oldest Known Communal Latrines Provide Evidence of Gregarism in Triassic Megaherbivores. *Sci. Rep.* **2013**, *3*, 3348. [[CrossRef](#)] [[PubMed](#)]
177. Green, J.L.; Schweitzer, M.H.; Lamm, E.-T. Limb Bone Histology and Growth in Placerias Hesternus (Therapsida: Anomodontia) from the Upper Triassic of North America. *Palaeontology* **2010**, *53*, 347–364. [[CrossRef](#)]
178. Viglietti, P.A.; Smith, R.M.H.; Compton, J.S. Origin and Palaeoenvironmental Significance of *Lystrosaurus* Bonebeds in the Earliest Triassic Karoo Basin, South Africa. *Palaeogeogr. Palaeoclimatol. Palaeoecol.* **2013**, *392*, 9–21. [[CrossRef](#)]
179. Mathewson, P.D.; Porter, W.P.; Barrett, L.; Fuller, A.; Henzi, S.P.; Hetem, R.S.; Young, C.; McFarland, R. Field Data Confirm the Ability of a Biophysical Model to Predict Wild Primate Body Temperature. *J. Therm. Biol.* **2020**, *94*, 102754. [[CrossRef](#)]
180. Huynh, T.T.; Poulsen, C.J. Rising Atmospheric CO₂ as a Possible Trigger for the End-Triassic Mass Extinction. *Palaeogeogr. Palaeoclimatol. Palaeoecol.* **2005**, *217*, 223–242. [[CrossRef](#)]
181. Hale, A.; Merchant, M.; White, M. Detection and Analysis of Autophagy in the American Alligator (*Alligator Mississippiensis*). *J. Exp. Zool. B Mol. Dev. Evol.* **2020**, *334*, 192–207. [[CrossRef](#)] [[PubMed](#)]
182. Grigg, G.; Beard, L. Hibernation by Echidnas in Mild Climates: Hints about the Evolution of Endothermy? In *Life in the Cold*; Springer: Berlin/Heidelberg, Germany, 2000; pp. 5–19.
183. Rial, R.V.; Akaärir, M.; Gamundí, A.; Nicolau, C.; Garau, C.; Aparicio, S.; Tejada, S.; Gené, L.; González, J.; De Vera, L.M.; et al. Evolution of Wakefulness, Sleep and Hibernation: From Reptiles to Mammals. *Neurosci. Biobehav. Rev.* **2010**, *34*, 1144–1160. [[CrossRef](#)] [[PubMed](#)]
184. Arad, Z. Physiological Responses to Increasing Ambient Temperature in Three Ecologically Different, Congeneric Lizards (Gekkoninae: *Ptyodactylus*). *Comp. Biochem. Physiol. A Physiol.* **1995**, *112*, 305–311. [[CrossRef](#)]
185. Li, C.; Wu, X.; Cheng, Y.; Sato, T.; Wang, L. An Unusual Archosaurian from the Marine Triassic of China. *Naturwissenschaften* **2006**, *93*, 200–206. [[CrossRef](#)]
186. Butler, R.J.; Brusatte, S.L.; Reich, M.; Nesbitt, S.J.; Schoch, R.R.; Hornung, J.J. The Sail-Backed Reptile *Ctenosauriscus* from the Latest Early Triassic of Germany and the Timing and Biogeography of the Early Archosaur Radiation. *PLoS ONE* **2011**, *6*, e25693. [[CrossRef](#)]
187. Romano, M.; Manucci, F. Resizing *Lisoivicia* Bojani: Volumetric Body Mass Estimate and 3D Reconstruction of the Giant Late Triassic Dicynodont. *Hist. Biol.* **2021**, *33*, 474–479. [[CrossRef](#)]
188. Ray, S.; Chinsamy, A. Functional Aspects of the Postcranial Anatomy of the Permian Dicyodont *Diictodon* and Their Ecological Implications. *Palaeontology* **2003**, *46*, 151–183. [[CrossRef](#)]
189. Botha-Brink, J. Burrowing in *Lystrosaurus*: Preadaptation to a Postextinction Environment? *J. Vertebr. Paleontol.* **2017**, *37*, e1365080. [[CrossRef](#)]
190. Angielczyk, K.D.; Steyer, J.-S.; Sidor, C.A.; Smith, R.M.H.; Whatley, R.L.; Tolan, S. Permian and Triassic Dicyodont (Therapsida: Anomodontia) Faunas of the Luangwa Basin, Zambia: Taxonomic Update and Implications for Dicyodont Biogeography and Biostratigraphy. In *Early Evolutionary History of the Synapsida*; Kammerer, C.F., Angielczyk, K.D., Fröbisch, J., Eds.; Vertebrate Paleobiology and Paleoanthropology; Springer Netherlands: Dordrecht, The Netherlands, 2014; pp. 93–138. ISBN 978-94-007-6841-3.
191. Kammerer, C.F.; Angielczyk, K.D. A Proposed Higher Taxonomy of Anomodont Therapsids. *Zootaxa* **2009**, *2018*, 1–24. [[CrossRef](#)]
192. Angielczyk, K.D.; Schmitz, L. Nocturnality in Synapsids Predates the Origin of Mammals by over 100 Million Years. *Proc. R. Soc. B Biol. Sci.* **2014**, *281*, 20141642. [[CrossRef](#)]
193. Wu, Y.; Wang, H.; Hadly, E.A. Invasion of Ancestral Mammals into Dim-Light Environments Inferred from Adaptive Evolution of the Phototransduction Genes. *Sci. Rep.* **2017**, *7*, 46542. [[CrossRef](#)] [[PubMed](#)]
194. de Souza Carvalho, I.; Campos, A.D.C.A.; Nobre, P.H. *Baurusuchus Salgadoensis*, a New Crocodylomorpha from the Bauru Basin (Cretaceous), Brazil. *Gondwana Res.* **2005**, *8*, 11–30. [[CrossRef](#)]
195. Guppy, M.; Fuery, C.J.; Flanigan, J.E. Biochemical Principles of Metabolic Depression. *Comp. Biochem. Physiol. Part B Comp. Biochem.* **1994**, *109*, 175–189. [[CrossRef](#)]
196. Withers, P.C.; Cooper, C.E. Metabolic Depression: A Historical Perspective. In *Aestivation*; Springer: Berlin/Heidelberg, Germany, 2010; pp. 1–23.
197. Mitchell, N.J.; Kearney, M.R.; Nelson, N.J.; Porter, W.P. Predicting the Fate of a Living Fossil: How Will Global Warming Affect Sex Determination and Hatching Phenology in Tuatara? *Proc. R. Soc. B Biol. Sci.* **2008**, *275*, 2185–2193. [[CrossRef](#)]
198. Mitchell, N.; Hipsey, M.R.; Arnall, S.; McGrath, G.; Tareque, H.B.; Kuchling, G.; Vogwill, R.; Sivapalan, M.; Porter, W.P.; Kearney, M.R. Linking Eco-Energetics and Eco-Hydrology to Select Sites for the Assisted Colonization of Australia's Rarest Reptile. *Biology* **2012**, *2*, 1–25. [[CrossRef](#)] [[PubMed](#)]
199. Raup, D.M.; Sepkoski, J.J. Mass Extinctions in the Marine Fossil Record. *Science* **1982**, *215*, 1501–1503. [[CrossRef](#)] [[PubMed](#)]